Parasite virulence in coinfected hosts: the importance of infection order

Aloïs Dusuel[1*], Luc Bourbon[2*], Emma Groetz[1], Nicolas Pernet[3], Mickaël Rialland[1], Benjamin Roche[4,5], Bruno Faivre[2], Gabriele Sorci[2#]

1. CTM - Center for Translational and Molecular Medicine, INSERM UMR 1231, Université de Bourgogne, 21000 Dijon, France ; LabEx LipSTIC, 21000 Dijon, France

2. Biogéosciences, CNRS UMR 6282, Université de Bourgogne, 6 Boulevard Gabriel, 21000 Dijon, France

3. Plateforme ImaFlow, Université de Bourgogne, Inserm, Institut Agro Dijon, CGFL, CHU Dijon Bourgogne, US58 BioSanD, F-21000 Dijon, France

4. MIVEGEC, IRD, CNRS, Université de Montpellier, 34090 Montpellier, France

5. International Joint Laboratory ELDORADO, IRD/UNAM, Mérida, Yucatán, México

#corresponding author: gabriele.sorci@u-bourgogne.fr

*equal contribution

Abstract

When hosts are simultaneously infected by different pathogens, the severity of the disease might be exacerbated compared to hosts harboring single infections. The reasons underlying these changes in parasite virulence are manifold. Here, we investigated the importance for the infection outcome of order and timing of infection. We used a model of rodent coinfection between two parasites that do not compete for common resources, an intestinal nematode (*Heligmosomoides polygyrus*) and an apicomplexan protozoan (*Plasmodium yoelii*). During single infections, *H. polygyrus* induced only mild disease symptoms. *Plasmodium* produced a substantial reduction in the number of red blood cells but all mice recovered from the infection. A different picture emerged in coinfected hosts. *Heligmosomoides* maintained a profile of mostly asymptomatic infection whatever the order of the infection (first or second). On the contrary, *P. yoelii* incurred substantially higher costs in hosts that had been previously infected with *H. polygyrus* (independently of the timing of infection). We then investigated the possible reasons underlying the increase of *Plasmodium* virulence in coinfected hosts. We found that coinfected hosts were less able to control *Plasmodium* multiplication and to recover from infection-induced anemia. Coinfected hosts had similar levels of erythropoietin and similar renewal of lost red blood cells, resulting in decreased tolerance to *Plasmodium* infection. Experimental administration of erythropoietin in coinfected hosts, partially decreased the severity of disease symptoms and improved tolerance. The detoxification of free heme released during the lysis of red blood cells, and the expression of Th1 and anti-inflammatory cytokine genes were also similar between coinfected and single infected hosts. However, coinfected mice had higher proportions of regulatory T cells expressing the CTLA-4 immune checkpoint, suggesting an enhanced immunosuppressive activity of Tregs. *Plasmodium* infection also induced the exhaustion of $CD8^+$ T cells, as coinfected mice had higher proportions of both PD-1^+ and LAG-3^+ $CD8^+$ T cells, and an increase in the $CD4^+/CD8^+$ ratio. Overall, these results stress the importance of the order of infection as a major determinant of disease severity in coinfected hosts. We discuss the possible epidemiological and evolutionary consequences of these results.

Keywords: coinfection, helminths, *Plasmodium*, nematodes, virulence

Introduction

Coinfection is a widespread phenomenon in plants, wildlife, livestock and humans (Viney and Graham 2013), and describes the occurrence of different parasites/pathogens (hereafter we will use the term parasite as a general term) at the same time in the same individual host. Coinfection has the potential to change the two principal drivers of the infection dynamics, the within host multiplication and the between host transmission (Wait et al. 2021; Imrie et al. 2023), and therefore parasite fitness (Clay and Rudolf 2019) and virulence (i.e., infection-induced damage) (Alizon et al. 2013). During single infections, parasites might have a better access to host resources, while during coinfection, access to resources might be limited if competing parasites share the same infection site or consume the same host resources (Graham 2008; Griffiths et al. 2015). This might affect the within host multiplication rate (for parasites that do multiply within the host) and the transmission rate if coinfection reduces the number of propagules produced per unit of time. This bottom-up regulation of coinfecting parasites might also change the cost paid by the host (e.g., Szabo et al. 2024) if, for instance, the overall host resource consumption exceeds the consumption during single infections. In this case, parasite fitness can also be jeopardized if coinfection compromises the survival of the host. The regulation of the coinfection dynamics might also involve top-down mechanisms, where parasites strive to exploit the host in the face of the immune defenses deployed by the host (Graham 2008). Under this scenario, depending on the nature of the coinfecting parasites, coinfection can have protective [when, for instance, coinfecting parasites elicit similar immune effectors (Filbey et al. 2019)] or antagonistic effects on the host ability to clear the infection (Shen et al. 2019). Specifically, top-down regulation of coinfecting parasites might be compromised when different immune effectors are involved in the process of parasite clearance. Broadly speaking, this is usually the case when hosts are simultaneously infected with microparasites that elicit a Th1 immune response (e.g., viruses and protozoa) and macroparasites that induce a Th2 response (e.g., helminths) (Supali et al. 2010; Ezenwa and Jolles 2011; Ma et al. 2020).

71 Coinfection between micro and macroparasites is a public health issue in several countries of
72 the intertropical areas, given the high prevalence of helminthiases in humans and the overlap with the
73 endemicity of major infectious diseases, such as malaria or AIDS (Webb et al. 2012; Afolabi et al. 2021).
74 Coinfection between gastrointestinal helminths and malaria has attracted attention in the last decades
75 not only to understand if and how helminths might aggravate the severity of malaria symptoms
76 (Degarege et al. 2016; Kwan et al. 2018), but also to forecast the public health effect of deworming
77 campaigns on malaria incidence and severity (Fenton 2013; Budischak et al. 2018), or to assess the
78 potential effect of helminth infection on the efficacy of malaria vaccines (Su et al. 2006; Noland et al.
79 2010; Coelho et al. 2019). However, despite considerable effort, epidemiological studies overall report
80 an inconsistent pattern where coinfection can both result in protection or increased severity of malaria
81 symptoms (Nacher 2011; Salazar-Castañón et al. 2014; Degarege and Erko 2016). This inconsistency
82 can be explained by several factors related, for instance, to the species of coinfecting helminths
83 (Adegnika and Kremsner 2012; Hürlimann et al. 2019). Work conducted using animal models has also
84 reported inconsistent results, depending on mouse strains and parasite species (Segura et al. 2009;
85 Knowles 2011; Kolbaum et al. 2012). Here, we suggest that a previously underestimated factor shaping
86 the outcome of the coinfection might also be the order and timing of the infection with the two
87 parasites (Salazar-Castañón et al. 2018; Karvonen et al. 2019; Billet et al. 2020). In most epidemiological
88 studies, the order of infection is not taken into account because this information is typically not
89 available and might contribute to inflate the heterogeneity of the reported results.
90 The rationale underlying the hypothesis that order of infection is an important driver of the
91 coinfection dynamics rests on the observation that, when coinfecting parasites are regulated through
92 top-down effects, the polarization of the host immune response following the first infection (Hartgers
93 and Yazdanbakhsh 2006; Kotepui et al. 2023) offers a favorable ground for the subsequent infection
94 with the second parasite (Su et al. 2005; Craig and Scott 2017). We explored this question using a
95 model of coinfection with the gastrointestinal nematode *Heligmosomoides polygyrus* (hereafter Hp)
96 and *Plasmodium yoelii* (hereafter Py) in mice. Hp is a model species in immunoparasitology (Reynolds

97 et al. 2012). This nematode is a natural parasite of rodents (Gregory et al. 1992) which elicits a
98 canonical Th2 immune response, orchestrated by Th2 cytokines, such as IL-4, IL-5 and IL-13 (Reynolds
99 et al. 2012). Mice are infected when ingesting infective larvae (L3), and adult worms live in the lumen
100 of the small intestine where they feed on the host's intestinal tissue (Bansemir and Sukhdeo 1994). Py
101 is also a model species for the study of the pathogenesis of malaria and the associated immune
102 response (Olatunde et al. 2022). The strain 17XNL of Py produces self-resolving infections, and
103 although the parasitemia can reach high level, all mice recover from the infection in about four weeks.
104 The cycle in the vertebrate host includes an early hepatic-stage that is followed by the asexual
105 replication within the red blood cells (RBCs) (blood-stage); the lysis of RBCs induces anemia, the typical
106 symptom of malaria infection. Infection with Py stimulates the production of pro-inflammatory
107 cytokines, such as the interferon-gamma (IFN-γ), and therefore polarizes the immune response
108 towards Th1 effectors (Olatunde et al. 2022).

109 Therefore, given that Hp and Py do not share the same ecological niche and do not share
110 common resources for their replication (RBCs for Py), or survival/reproduction (intestinal lumen for
111 Hp), any interference between the two parasites is unlikely to be driven by bottom-up regulation
112 mechanisms. On the contrary, given that the two parasites elicit different immune effectors, and that
113 Th1 and Th2 cytokines have reciprocal inhibitory effects (Paludan 1998), top-down mechanisms are
114 likely candidates to drive the outcome of the coinfection in this system.

115 We conducted a series of experiments with the aim of exploring to what extent the order and
116 timing of the infection with the two parasites drives the infection dynamics and the severity of the
117 disease. We also explored the possible mechanisms underlying the increased disease severity in
118 coinfected hosts. Based on the rationale reported above, we predicted that if the polarization of the
119 immune response towards Th1 (in the case of Py infection) or Th2 (in the case of Hp infection) makes
120 the host more vulnerable to the infection with the other parasite, coinfection should aggravate the
121 symptoms of the disease, compared to single infections.

122

123 **Materials and Methods**

124 *Ethical statement*

125 Experiments were approved by the Comité d'éthique Grand Campus Dijon of the University of
126 Burgundy and were authorized by the French Ministry of Higher Education and Research under the
127 numbers 33492 and 47573.

128 *Experimental animals and infections*

129 C57BL/6JRj female mice (7-10 weeks old) were purchased from Janvier Labs (Le Genest-Saint-
130 Isle, France), housed in cages containing 5 individuals under pathogen-free conditions, and maintained
131 under a constant temperature of 24°C and a photoperiod of 12h:12h light:dark with *ad libitum* access
132 to water and standard chow diet (A03-10, Safe, Augny, France). All mice were acclimatized to the
133 housing conditions during, at least, 7 days prior to the start of the experiments, were monitored twice
134 a day to check health status, and euthanized by cervical dislocation under anesthesia with isoflurane
135 either if they reached previously defined end points (and considered as mortality events in the survival
136 analysis) or at specific days post-infection (p.i.) for terminal collection of blood and organs (and
137 considered as censored events in the survival analysis).

138 Mice were infected with *Plasmodium yoelii* 17XNL by intra-peritoneal (i.p.) injection with $5x10^5$
139 infected red blood cells (iRBC) suspended in 0.1 ml of PBS and/or *Heligmosomoides polygyrus bakeri*
140 by oral gavage with L3 larvae (350 larvae suspended in 0.2 ml of drinking water).

141 *Experimental groups*

142 Mice were randomly assigned to 8 experimental groups (15 to 20 mice per group) as described
143 in figure 1. A control group (group 1) of mice was sham infected (i.p. injection of 0.1 ml of PBS and oral
144 gavage with a 0.2 ml of drinking water). Two groups (groups 2 and 3) received single infections, either
145 with Hp or Py. Five additional groups were coinfected with the two parasites according to specific
146 orders and timings of infection. In one group, mice were simultaneously infected with the two
147 parasites (group 4); in two groups, mice were infected first with Hp and subsequently infected with Py
148 either at day 7 post Hp infection, or at day 28 post Hp infection (groups 5 and 6); in two groups, mice

149 were first infected with Py and subsequently infected with Hp either at day 14 post Py infection, or at
150 day 28 post Py infection (groups 7 and 8). The timings of infection in the coinfection groups correspond
151 to specific stages in the life cycles of the two parasites. Day 7 and 28 post Hp infection correspond to
152 the stage that just precedes the emergence of the adult worms in the intestinal lumen and when the
153 infection has reached a chronic stage, respectively. Day 14 and day 28 post Py infection approximately
154 correspond to the parasitemia peak and the end of the acute phase infection, respectively. The whole
155 experiment was repeated twice, although not all traits were measured in all mice of the two replicates.

156 *Erythropoietin administration*

157 Mice (n = 20) were infected with Hp and at day 28 p.i. they were infected with Py. Mice were
158 then split randomly into two groups, one received an i.p. injection of 1 µg of recombinant mouse
159 erythropoietin (rEPO) (959-ME, Bio-Techne, Minneapolis, Minnesota, USA) in 200 µl of PBS at days 0,
160 2 and 4 post Py infection; the other group was injected with 200 µl of PBS only, for control.

161 *Monitoring of health status, hematological and plasma parameters, and Py parasitemia*

162 Mice were regularly weighed (at least three times a week) and body mass was used as an
163 integrative marker of host health. Hematological parameters were assessed by collecting 10 µl of blood
164 from the tail tip in 0.5 ml tubes with 1 µl of heparin (Héparine Choay® 25 000 UI/5ml, Sanofi-Aventis,
165 Gentilly, France). These samples were immediately read with a SCIL Vet abc Plus+ hematology analyzer
166 (Horiba Medical, Montpellier, France) to assess RBC concentration and mean globular volume. For
167 mice with Py infection, a drop of blood was smeared on a slide and fixed with methanol. Slides were
168 subsequently stained with a Giemsa RS solution (Carlo Erba Reagents, Val de Reuil, France) (10% v/v in
169 phosphate buffer) for 15 minutes and rinsed with water. Infected RBCs were counted using an optical
170 microscope under magnification x1000, and parasitemia expressed as the proportion of iRBCs.

171 At day 3, 14, 21 and 35 p.i. (post second infection for the coinfection groups), five mice per
172 group were euthanized by cervical dislocation under isoflurane anesthesia, for terminal collection of
173 total peripheral blood and organs. Given the severity of the disease symptoms, the simultaneous
174 infection group and the two coinfection groups first infected with Hp (groups 4, 5, 6) were only

175 monitored up to day 21 post Py infection. Plasma was separated from total blood by centrifugation (7
176 min 3000 rpm 4°C), aliquoted and stored at -80°C.

177 Plasma levels of aspartate aminotransferase (AST) and heme oxygenase-1 (HO-1) were
178 assessed with ab263882 and ab229431 commercial ELISA kits from Abcam (Cambridge, UK),
179 respectively. Plasma levels of mouse erythropoietin (EPO) were assessed with EM28RB commercial
180 ELISA kit from Invitrogen™ (Carlsbad, California, USA). Plates were read with a SpectraMax iD3 multi-
181 mode microplate reader (Molecular Devices, San Jose, California, USA).

182 *Organ collection*

183 Spleen was removed and weighed. About one third of the spleen was cut and immediately
184 frozen in liquid nitrogen for RT-qPCR, and the remaining was kept on ice in PBS before the flow
185 cytometry staining procedure. A liver slice (left lobe) was also immediately frozen in liquid nitrogen for
186 RT-qPCR.

187 *RNA extraction and qPCR for Hmox-1, IFN-γ, IL-10 and TGF-β1 gene expression*

188 Tissues were homogenized in TRIzol™ Reagent (Invitrogen™, Carlsbad, California, USA) under
189 strong agitation using 0.5 mm glass beads and a Precellys® 24 Touch homogenizer (Bertin
190 Technologies, Montigny-le-Bretonneux, France). RNA extraction was performed following the
191 manufacturer's instructions. RNA concentration was measured with a NanoPhotometer® N50 (Implen,
192 Munich, Germany). Reverse transcription was performed with a High-Capacity cDNA Reverse
193 Transcription Kit (Applied Biosystems™, Foster City, California, USA) from 1.5 µg total RNA.
194 Quantitative PCR was performed with PowerUp™ SYBR™ Green Master Mix (Applied Biosystems™) on
195 a QuantStudio™ 3 Real-Time PCR System (Applied Biosystems™). We used two housekeeping genes (β-
196 actin and GAPDH); β-actin provided more consistent values (less intra-group variability) and therefore
197 we used it as the reference gene. Primer sequences are reported in the supplementary material (table
198 S1), and were checked for specificity using the Primer-BLAST tool (NCBI). Melt curve analysis was also
199 performed in all samples to check for the presence of nonspecific amplification products.

200

201 *Spectral flow cytometry*

202 Spleens were homogenized with a 70 µm cell strainer and washed two times with PBS to obtain
203 a single-cell suspension. RBCs were removed from suspensions with eBioscience™ RBC Lysis Buffer
204 (Invitrogen™) (3 min incubation at RT). Cells were counted with viability trypan blue dye and
205 dispatched in 96-well V bottom plates to obtain $1x10^7$ live cells/well. Cells were then stained with
206 LIVE/DEAD™ Fixable Blue Dead Cell Stain Kit (Invitrogen™) in PBS for 30 min at 4°C, incubated in stain
207 buffer with BD Fc Block™ (BD Pharmingen™, Franklin Lakes, New Jersey, USA) for 15 min at RT (0.5
208 µg/well), and stained with surface antibodies in brilliant stain buffer (see table S2 for details on the
209 markers used) for 30 min at 4°C. Cells were then fixed and permeabilized with eBioscience™ Foxp3 /
210 Transcription Factor Staining Buffer Set (Invitrogen™) prior intracellular staining in brilliant stain buffer
211 (table S2) for 30 min at RT. Cells were resuspended in stain buffer, filtered with 100 µm nylon mesh
212 and analyzed on a 4-lasers (UV/V/B/R) Aurora™ (Cytek® Biosciences, Fremont, California, USA) spectral
213 flow cytometer in the ImaFlow Facility, part of the US58 BioSanD. Events were gated and analyzed with
214 SpectroFlo® v3.0.0 software (Cytek® Biosciences) (see figures S1 and S2 for the gating strategy).

215 *Statistical analyses*

216 We used general and generalized linear mixed models (GLMM) to analyze data where each
217 individual mouse was repeatedly sampled, using either a normal distribution or a beta distribution (i.e.,
218 for proportions) of errors. Mouse ID was included in these models as a random intercept. Variables do
219 not necessarily vary linearly with time over the course of the infection. We therefore included squared
220 (and cubic) time p.i. to capture these nonlinear relationships. However, polynomial regression might
221 provide a poor fit to the data. Therefore, we also ran general additive models (GAM) where the degrees
222 of freedom of the smoothing function were chosen based on the generalized cross-validation (GCV)
223 optimization criterion. Some variables had an asymmetrical distribution and were log-transformed to
224 reduce skewness and meet the model assumptions.

225 Differences in survival between groups were analyzed using the Kaplan Meier estimator and
226 significance assessed using a Log-Rank test. For coinfected mice, any mortality that had occurred

227 before the infection with the second parasite was considered as caused by single infections (and
228 therefore included as single infected individuals in the model); any effect of coinfection on survival
229 was, thus, assessed only after the infection with the second parasite. To increase the statistical power,
230 the survival analysis also included additional mice that were followed for a longer period of time (up
231 to day 99 p.i.) for other purposes (i.e., to assess the long-term effect of coinfection on the infection
232 dynamics). Therefore, the survival analysis included up to four replicated datasets.

233 For variables that were measured only once per individual mouse, we ran general or
234 generalized linear models (GLM), depending on the distribution of errors (normal or beta distribution).
235 Post-hoc comparisons between groups were done using LS-means with Bonferroni correction of p
236 values. Differences in sample size across groups reflect missing values, either due to the reaching of
237 the end point or to technical issues during the processing of the sample.

238 To simplify the interpretation of the results, we ran different sets of models, comparing
239 different groups. First, we compared non-infected mice versus single infections (groups 1, 2 and 3).
240 These models provided us with the baseline information on the intrinsic effect of each parasite when
241 infecting the host alone. Then, we compared single infection versus coinfection groups. This was done
242 separately for Py and Hp by including in the model the corresponding coinfection groups where Py and
243 Hp infected mice that had been previously infected with the other parasite (i.e., groups 3, 4, 5, 6 in one
244 model, and groups 2, 7, 8 in another model). The simultaneous infection group (group 4) was always
245 included in the Py model. Given that the timing of the infection did appear to have minor effects on
246 the response variables, we also ran models where the different coinfection groups were clustered
247 together (groups 4, 5 and 6; groups 7 and 8) and we compared non-infected, single infected and
248 coinfected hosts in the same model. Finally, we ran a model that was restricted to the coinfection
249 groups (excluding the simultaneous infection group) where we could assess the effect of the order of
250 the infection [either Hp first (groups 5 and 6), or Py first (groups 7 and 8)]. All the statistical analyses
251 and figures were done using SAS Studio.

252

253 **Results**

254 ***Severity of the disease in single and coinfected hosts***

255 *Body mass*

256 We analyzed body mass as percent variation relative to the body mass at the day of the sham-
257 infection for the control group (group 1) and the day of the infection for single and simultaneous
258 infection groups (groups 2, 3 and 4) or the day of the second infection for the coinfection groups
259 (groups 5, 6, 7 and 8). We first compared changes in body mass over time between non-infected and
260 single (Hp, Py) infected mice (groups 1, 2, 3). The model showed that body mass increased linearly over
261 time, at a similar rate for non-infected and single infected mice (table 1, fig. 2a). We then compared
262 changes in body mass in mice that were infected with Py alone and mice that were simultaneously
263 infected or were first infected with Hp and then with Py (groups 4, 5, 6). Although mice in the
264 coinfection groups lost body mass from day 14 post Py infection onwards (table S3, fig. S3a), the
265 squared time by treatment interaction was not statistically significant (table S3). Given that there was
266 no apparent difference in the dynamics of body mass change between the coinfection groups, we ran
267 an additional model where we compared the changes in body mass between non-infected, single Py
268 infected and coinfected groups together (groups 4, 5 and 6). This model showed a strong effect of
269 coinfection on changes in body mass (table 2, fig. 2b), with coinfected mice losing body mass over the
270 course of the infection.

271 A different picture emerged when comparing changes in body mass in mice that were infected
272 first with Py and then with Hp. In this case, coinfection (groups 7 and 8) slowed down the rate of body
273 mass gain, but did not produce a loss in body mass (table S4, fig. S3b). As the timing of infection did
274 not have any effect on the changes in body mass, we grouped them and ran an overall model
275 comparing non-infected, single Hp infected and coinfected groups (7 and 8) together. This model
276 confirmed the slight effect of coinfection on the dynamics of body mass change, with coinfected mice
277 having a slower rate of increase in body mass, but not losing mass over time (table 3, fig. 2c). Finally,
278 we ran a model that was only restricted to the four coinfection groups (groups 5, 6, 7 and 8) where

279 mice were either infected first with Hp or with Py. This model confirmed to importance of the order of
280 infection in shaping the dynamics of body mass (table S5, fig. 2d).
281 Therefore, coinfection aggravated one of the most integrative symptoms of disease severity,
282 but the magnitude of the aggravating effect was strongly dependent on the order of the infection.
283 *Splenomegaly*
284 Splenomegaly (i.e., the enlargement of the spleen) is another prominent symptom of the
285 infection with Hp or Py. We measured spleen mass at day 3, 14, 21 and 35 p.i. and confirmed that
286 single infection induced splenomegaly of different magnitude depending on the parasite (table S6, fig.
287 3a). When comparing groups infected first with Hp and then with Py (plus the simultaneous infection,
288 groups 4, 5, 6), coinfection only had a mild initial effect on splenomegaly at day 3 post Py infection
289 compared to single Py infected hosts (Table S7), but by day 14 p.i. the differences vanished (fig. S4a).
290 This result was corroborated when comparing non-infected, single Py infected and coinfected groups
291 together (Table S8, fig. 3b).
292 When comparing the effect of coinfection in groups that were first infected by Py (groups 7
293 and 8), we found only a moderate increase in spleen mass, essentially as a consequence of the residual
294 enlargement due to the previous Py infection, since the difference between single Hp infection and
295 coinfection groups tended to vanish over time (table S9 and table S10, fig. 3c).
296 The asymmetric effect of infection order on splenomegaly was best captured by the model on
297 the four coinfection groups (groups 5, 6, 7 and 8) where mice were either infected first with Hp or with
298 Py. This model showed that spleen mass increased over the course of the infection only when mice
299 were first infected with Hp and subsequently by Py (table S11, fig. 3d).
300 Therefore, as for body mass, coinfection affected splenomegaly in an asymmetric way,
301 depending on infection order.
302 *Marker of liver damage*
303 We compared a marker of liver damage (aspartate aminotransferase, AST) in plasma at day 21
304 p.i. in non-infected and single (Hp, Py) infected mice, and found that Py infected mice had moderately

305 higher levels of AST compared to non-infected hosts (GLM, $F_{2,23} = 4.45$, $p = 0.0218$, n = 26 individuals;
306 fig. 4a). Coinfection did aggravate liver damage in the groups where Py followed the Hp infection (plus
307 simultaneous infection, groups 4, 5, 6) (GLM, $F_{3,36} = 4.28$, $p = 0.0111$, n = 40; fig. S5a), and this effect
308 was confirmed when analyzing non-infected, single Py infected and coinfected mice together in the
309 same model (GLM, $F_{2,45} = 4.22$, $p = 0.0209$, n = 48; fig. 4b).

310 We found rather similar effects of coinfection when analyzing the groups where Hp follows Py
311 (groups 7 and 8), with coinfection groups having higher AST levels compared to non-infected and single
312 Hp infected groups (GLM, $F_{2,29} = 4.96$, $p = 0.0141$, n = 32; fig. 4c, fig. S5b). As a consequence, there was
313 no effect of infection order in the coinfection groups (groups 5, 6, 7 and 8) on AST level at day 21 p.i.
314 (GLM, $F_{1,35} = 0.28$, $p = 0.5976$, n = 37; fig. 4d).

315 *Survival*

316 In agreement with the pattern of change in body mass over the course of the infection, we did
317 not find any difference in the survival rate between non-infected and single infected mice (Log-Rank
318 test $\chi^2_2 = 0.92$, $p = 0.6315$, n = 229; fig. 5a). Timing of infection did not affect host survival in coinfected
319 groups when Py followed the Hp infection (plus simultaneous infection, groups 4, 5 and 6) (Log-Rank
320 test $\chi^2_2 = 1.45$, $p = 0.4844$, n = 148; fig. S6), we therefore compared the coinfection groups together
321 with the non-infected and single Py infection and found a strong effect of coinfection (Log-Rank test
322 $\chi^2_2 = 26.02$, $p < 0.0001$, n = 282; fig. 5b).

323 There was no host mortality in the coinfection groups where Hp followed Py (groups 7 and 8),
324 whatever the timing of the infection. Therefore, there was no difference in the mortality rate of non-
325 infected, single Hp infected and coinfected groups (groups 7 and 8) (Log-Rank test $\chi^2_2 = 2.34$, p =
326 0.3099, n = 229; fig. 5c). As a consequence, order of infection was a strong predictor of host mortality
327 in the coinfection groups (groups 5, 6, 7 and 8) (Log-Rank test $\chi^2_1 = 13.47$, $p = 0.0002$, n = 189; fig. 5d).

328 Overall, these results show that order of infection has a paramount effect on the severity of
329 the symptoms and therefore on parasite virulence (infection-induced damage), with Hp infection
330 producing mild symptoms whatever the order of the infection, and Py becoming substantially more

331 virulent when infecting hosts already harboring the nematode. However, the timing of infection had
332 virtually no effect on disease severity.

333 ***Py parasitemia***

334 If previous infection with Hp makes the ground more favorable for a subsequent Py infection,
335 we should expect higher parasitemia in coinfected hosts (groups 4, 5, 6) compared to single Py
336 infection. During single infection, parasitemia reached a peak at around day 16 p.i., and then the
337 infection resolved by day 30 (fig. 6a; fig. S7). Given that the coinfection groups (groups 4, 5 and 6) were
338 stopped at day 21 p.i., we could only compare the rising and the early declining stages of the
339 parasitemia. The model showed that coinfected groups reached higher parasitemia and that, contrary
340 to the single infection group, the parasitemia of coinfected mice kept increasing up to day 21 p.i. (table
341 S12 and table 4, fig. S8 and fig. 6b).

342 Therefore, as expected, previous infection with Hp made a more favorable ground for
343 subsequent Py infection that replicated more and for longer time in coinfected mice. Enhanced
344 persistent parasitemia might thus explain the observed increase of Py virulence in coinfected hosts
345 through specific costs incurred during the asexual reproduction of Py.

346 ***Specific costs of Py infection***

347 The principal cost induced by Py infection is related to the anemia caused by the lysis of RBCs
348 during the asexual reproduction of the parasite (Olatunde et al. 2022). We therefore assessed the
349 changes in RBC counts over the course of the infection. First, we compared changes in RBC counts
350 between non-infected and single (Hp, Py) infections. As expected, Py infection produced a sharp
351 decline in the number of RBCs, while there was no difference between non-infected and Hp single
352 infection (table 5, fig. 7a, fig. S9), corroborating the idea that Py and Hp do not compete for common
353 resources.

354 Coinfected groups (groups 4, 5, 6) had a similar drop in the count of RBCs (table S13, fig. S10),
355 and we clustered them and compared the changes in RBC counts between non-infected, single Py
356 infected and coinfected mice (groups 4, 5, 6). The model showed that coinfected mice still had low

357 levels of RBCs at day 21 p.i. compared to single Py infected mice that had already started the recovery
358 phase (table 6, fig. 7b, fig. S10c).

359 Infection-induced anemia stimulates erythropoiesis with the aim of restoring homeostatic RBC
360 counts. We therefore investigated whether coinfection impaired the host capacity to repair the
361 damage (here the loss of RBCs) caused by the infection. To this purpose, we assessed the production
362 of erythropoietin (EPO) (at day 14 and 21 p.i.) and the mean globular volume (MGV) that reflects the
363 proportion of reticulocytes among the total RBCs.

364 Mice with single Py infection produced EPO in response to the loss of RBCs compared to non-
365 infected individuals (GLM, $F_{1,34} = 113.53$, $p < 0.0001$, n = 38; fig. 7c). However, despite having lower
366 RBC counts, coinfected hosts (groups 4, 5, 6) did not produce more EPO compared to single Py infected
367 mice, neither when including each coinfection group separately in the model (GLM, $F_{3,67} = 2.24$, p =
368 0.0917, n = 75; fig. S11), nor when grouping them (post hoc comparison of LS-means between single
369 infection and coinfection with Bonferroni correction, p = 0.3096, n = 94; fig. 7c)

370 This result was mirrored by the change of MGV over the course of the infection. Py infected
371 mice had a sharp increase in the MGV between day 11 and 21 p.i., compared to non-infected and Hp
372 infected mice, indicating a higher proportion of reticulocytes among RBCs (table 7, fig. 7d, fig. S12).
373 However, changes in MGV were similar between single Py infection and the coinfection groups (groups
374 4, 5, 6) (table 8, fig. 7e, table S14, fig. S13).

375 Given that coinfected hosts harbored more parasites than single infected hosts, a similar rate
376 of renewal of lost RBCs should result in a reduction in tolerance in coinfected mice. We defined
377 tolerance as the slope of the regression of RBC counts on parasitemia, the steeper the slope the weaker
378 the tolerance (i.e., the capacity to cope with the damage induced by the infection). As expected, we
379 found that coinfected hosts were less tolerant (i.e., steeper slope) to Py infection compared to single
380 infected mice (table 9; fig. 7f).

381 If coinfected hosts suffer from more severe disease symptoms because they cannot effectively
382 restore RBCs lost during the infection, we should expect that experimentally inducing erythropoiesis

383 might, at least partially, dampen the cost of coinfection. To explore this hypothesis, we ran an
384 experiment where mice were first infected with Hp and after 28 days they were infected with Py. These
385 coinfected mice were then treated with a rEPO or left as control. We assessed the severity of the
386 symptoms using an integrative marker of health (body mass), a specific marker of Py infection (changes
387 in RBCs), and any mortality (reaching of the end points) that might have occurred during the course of
388 the infection.

389 As predicted, treating coinfected mice with rEPO reduced the severity of the disease
390 symptoms, since body mass remained stable over the course of the infection, while mice in the control
391 group lost body mass from day 14 p.i. onwards (table 10, fig. 8a). rEPO treatment only slightly affected
392 anemia (GLMM, time p.i.*treatment, $F_{1,129} = 4.12$, $p = 0.0443$, n = 20 individuals and 153 observations;
393 fig. 8b, fig. S14), and although mortality was higher in the control group, the difference was not
394 statistically significant (Log-rank test, $\chi^2_1 = 1.059$, $p = 0.3034$, n = 20; fig. 8c), suggesting that other
395 aspects of the pathophysiology of coinfection might explain the observed increase in Py virulence.
396 Nevertheless, the rEPO administration improved the tolerance to Py infection, since coinfected mice
397 treated with rEPO had similar slope relating RBC counts to parasitemia as single Py infected hosts
398 (GLMM, treatment*parasitemia, $F_{1,111} = 0.11$, $p = 0.7363$, n = 25 individuals and 138 observations; fig.
399 8d). Therefore, coinfection reduced the tolerance to Py infection and administering rEPO partially
400 restored it.

401 In addition to inducing anemia, the lysis of RBCs releases free heme groups that have pro-
402 oxidant and pro-inflammatory properties, and stimulates the production of enzymes whose role is to
403 scavenge them. We therefore hypothesized that the increased virulence of Py in coinfected hosts
404 (when Py follows Hp) might stem from an impaired capacity to detoxify free heme groups. To this
405 purpose, we assessed the expression of the *Hmox1* gene in splenocytes at day 14 p.i. and the amount
406 of circulating heme oxygenase-1 (HO-1) in plasma at day 14 and 21 post-infection. *Hmox1* was strongly
407 upregulated in Py infected mice compared to non-infected individuals (GLM, $F_{1,8} = 96.92$, n = 10; $p <$
408 0.0001; fig. 9a, fig. S15a), and it was also upregulated in coinfected groups (groups 4, 5, 6) compared

409 to single Py infected hosts (post-hoc comparison of LS-means, p = 0.0074, n = 28; fig. 9a, fig. S15a,b).
410 However, although single Py infected mice also had much higher plasma levels of the enzyme HO-1 at
411 both day 14 and 21 p.i. compared to non-infected individuals (GLM, $F_{1,24}$ = 82.98, p < 0.0001, n = 28;
412 fig. 9b), coinfected groups (groups 4, 5, 6) did not differ from single Py infection (when considering the
413 different coinfection groups separately, GLM, $F_{3,68}$ = 2.49, p = 0.0677, n = 76; fig. S15c; when
414 considering the coinfection groups together, post-hoc comparison of LS-means, p = 1, n = 86; fig. 9b).
415 Therefore, although *Hmox1* gene expression was upregulated in the coinfection groups, the level of
416 the enzyme in the blood did not differ between single infection and coinfection.

417 Another important function related to the clearance of free hemoglobin is provided by the
418 scavenger receptor CD163 expressed on red pulp macrophages (RPM, F4/80$^+$ CD11b$^-$) (Kristiansen et
419 al. 2001). We therefore assessed the proportions of RPM that were CD163$^+$, by flow cytometry, and
420 compared them between non-infected and single Py infected and found that the population of CD163$^+$
421 RPM drastically dropped during the infection (generalized linear model with a beta distribution of
422 errors, $F_{1,35}$ = 344.88, p < 0.0001, n = 39; fig. 9c). However, the proportion of RPM that were CD163$^+$
423 was similarly reduced in coinfected mice (groups 4, 5, 6) compared to single Py infection, at both day
424 14 and 21 p.i. (LS-means comparison with Bonferroni correction, day 14 p.i., p = 0.1648, day 21 p.i., p
425 = 0.1959, n = 100; fig. 9c, fig. S15d). The receptor CD163 was also less expressed in F4/80$^+$ CD11b$^-$ of
426 Py infected mice, as shown by the drastic drop in mean fluorescence intensity (MFI), with no difference
427 between single and coinfected mice (LS-means comparison with Bonferroni correction, day 14 p.i., p =
428 1, day 21 p.i., p = 1, n = 100; fig. 9d). Therefore, the population of CD163$^+$ RPM which are a key resident
429 cell population responsible for clearing free hemoglobin released during the lysis of RBCs similarly
430 decreased in single and coinfected mice.

431 ***Immune predictors of Py virulence***

432 *Plasmodium* infection elicits proinflammatory effectors that might cause immunopathology if
433 regulatory mechanisms fail to restore homeostasis. Therefore, we speculated that exacerbated disease
434 severity in coinfected hosts (when Py follows Hp) might stem from an overreacting, non-regulated,

435 inflammatory response. To address this question, we first assessed the gene expression of pro- and
436 anti-inflammatory cytokines in splenocytes at day 3 and 14 post-infection. IFN-γ, IL-10 and TGF-β1
437 genes were all overexpressed at both 3 and 14 days p.i. in single Py infected hosts compared to non-
438 infected mice (GLM, IFN-γ, $F_{1,34} = 24.44$, $p < 0.001$; IL-10, $F_{1,34} = 49.86$, $p < 0.001$; TGF-β, $F_{1,34} = 20.62$, p
439 < 0.001, n = 38; fig. 10; fig. S16a,b,c). However, coinfection (groups 4, 5, 6) did not induce a change in
440 the expression of any of the genes compared to single Py infection (LS-means comparison with
441 Bonferroni correction, all p's = 1, fig. 10, fig. S16d,e,f). Previous work conducted on the same model
442 system has shown that coinfected mice have a higher activation of regulatory T cells (Treg), possibly
443 accounting for their impaired anti-*Plasmodium* response (Tetsutani et al. 2009). Therefore, we
444 assessed the proportions of $CD4^+$ T cells that were $FoxP3^+$ by flow cytometry and compared them, over
445 the course of the infection, between non-infected, single Py infected and coinfected mice (groups 4,
446 5, 6); we found no differences between single Py infection and coinfection groups (LS-means
447 comparison with Bonferroni correction, p = 1; n = 100; fig. 11a, table S15; fig. S17a). The expression of
448 the immune check point CTLA-4 on Treg has been shown to impede immunity to the acute infection
449 with Py (Kurup et al. 2017), by enhancing their immunosuppressive activity. We thus assessed the
450 proportions of $CD4^+$ T cells that were $FoxP3^+$ and CTLA-4^+ by flow cytometry and compared them
451 between non-infected, single Py infected and coinfected mice (groups 4, 5, 6); we found that
452 coinfected mice had a higher proportion of CTLA-4^+ Treg compared to non-infected and single Py
453 infection at day 14 p.i. (table 11; fig. 11b; table S16; fig. S17b). Therefore, although coinfection did not
454 produce an expansion of the Treg population compared to single Py infected hosts, the
455 immunosuppressive power of Treg was upregulated in coinfected hosts.

456 Using flow cytometry, we also immunophenotyped mice using a large panel of markers in the
457 spleen (table S2), at day 3, 14 and 21 post-infection. We identified 20 cell populations (table S17) and
458 their proportions were included as variables in a principal component analysis (PCA), with a PCA per
459 sampling day. The first two components explained 29.02% and 18.79%, 39.65% and 12.86%, 37.63%
460 and 15.92% of the total variance, at day 3, 14, and 21 p.i., respectively. The correlation circles showed

461 that many of the variables included in the PCA had high absolute loadings (table S17, fig. 12a, b, c), and
462 effectively discriminated the three experimental groups (non-infected, single Py infected and
463 coinfected mice) over the course of the infection (fig. 12d,e,f).

464 At day 3 p.i., the scores along the first principal component (PC1) strongly differed between
465 the three experimental groups (GLM, $F_{2,45} = 28.56$, n = 48; $p < 0.0001$), with coinfected mice (groups 4,
466 5, 6) having higher scores compared to both non-infected and single Py infection (LS-means
467 comparisons with Bonferroni correction, both p's < 0.0001; fig. 12g). At day 14 and 21 p.i., there was
468 a complete separation, along the PC1, between the three groups, with single Py infected lying in
469 between non-infected and coinfected individuals (groups 4, 5, 6) (day 14 p.i.: GLM, $F_{2,43} = 313.37$, $p <$
470 0.0001, n = 46; day 21 p.i.: GLM, $F_{2,51} = 257.50$, $p < 0.0001$, n = 54; fig. 12g). The PC2 had a much less
471 discriminant power among groups (day 3 p.i.: GLM, $F_{2,45} = 3.02$, $p = 0.0588$, n = 48; day 14 p.i.: GLM,
472 $F_{2,43} = 1.27$, $p = 0.2902$, n = 46; day 21 p.i.: GLM, $F_{2,51} = 7.57$, $p = 0.0013$, n = 54; fig. 12h).

473 To go further, we focused on the variables that had strong absolute loadings on the PC1 and
474 compared them between the groups, with the aim to see if there was a consistent difference between
475 single Py infected and coinfected hosts (groups 4, 5, 6). The proportion of Th2 (proportion of $CD4^+$ T
476 cells that were GATA-3^+) differed between single and coinfected hosts at the three sampling dates
477 (GLM with a beta distribution of errors, $F_{2,139} = 53.91$, $p < 0.0001$, n = 148; LS-means comparison
478 between single and coinfected with Bonferroni correction, day 3, $p = 0.0002$; day 14, $p = 0.0102$; day
479 21, $p < 0.0001$; fig. 13a). Among the other variables, only $CD8^+$ T cells consistently discriminated
480 between single Py and coinfected hosts (groups 4, 5, 6), with the proportion of $CD8^+$ T cells (proportion
481 of $CD3^+$ that were $CD8^+$) sharply decreasing over time and especially so in coinfected hosts (GLM with
482 a beta distribution of errors, $F_{2,139} = 347.41$, $p < 0.0001$, n = 148; LS-means comparison between single
483 and coinfected with Bonferroni correction, day 3, $p = 1$; day 14, $p < 0.0001$; day 21, $p < 0.0001$, fig.
484 13b).

485 Therefore, Th2 and $CD8^+$ T cells were the two cell populations that best discriminated between
486 Py infected and coinfected hosts (when Py follows Hp). While the effect of coinfection on the rise of

487 Th2 lymphocytes can easily be understood as the direct consequence of Hp induction of Th2 immunity,
488 we wished to better investigate the reasons underlying the decrease of $CD8^+$ T cells in coinfected mice.
489 To this purpose, we assessed the proportion of $CD8^+$ T cells that expressed three immune checkpoints
490 in non-infected, single Py infected and coinfected hosts (groups 4, 5 and 6), and predicted that
491 coinfected mice should have higher proportions of $CD8^+$ T cells expressing the immune checkpoints
492 compared to single infection. Infection enhanced the proportion of CTLA-4^+ $CD8^+$ T cells (proportion of
493 $CD8^+$ that were CTLA-4^+) but there was no difference between single infection and coinfection at any
494 of the sampling day (GLM with a beta distribution of errors: day 14 p.i, t = -0.52, df = 90, p = 1; day 21
495 p.i., t = -1.19, df = 90, p = 1; fig. 14a). The proportions of LAG-3^+ $CD8^+$ and PD-1^+ $CD8^+$ cells (proportion
496 of $CD8^+$ that were LAG-3^+ and PD-1^+, respectively) were also increased in infected mice compared to
497 non-infected individuals, however, at day 14 p.i. there was also a higher proportion of LAG-3^+ and PD-
498 1^+ $CD8^+$ T cells in coinfected mice compared to single infection (GLM with a beta distribution of errors:
499 LAG-3, day 14 p.i.: t = 3.38, df = 91, p = 0.0163; day 21 p.i., t = 2.36, df = 91, p = 0.3040; PD-1, day 14
500 p.i.: t = 3.94, df = 90, p = 0.0024; day 21 p.i., t = 2.26, df = 91, p = 0.3948, fig. 14b,c).

501 Persistent antigenic stimulation and high levels of inhibitory receptors (immune checkpoints)
502 can lead to the exhaustion of $CD8^+$ T cells, characterized by a loss of effector functions and proliferative
503 potential (McLane et al. 2019), that could explain the increase in the $CD4^+/CD8^+$ ratio above the
504 homeostatic value (between 1.5 and 2.5) (McBride and Striker 2017). Deviations from this homeostatic
505 value have been associated with severe symptoms in a few infectious diseases (e.g., Pascual-Dapena
506 et al. 2022). We therefore wished to investigate if high values of the $CD4^+/CD8^+$ ratio also predicted
507 mortality in our system. We could not investigate this point at the individual level because data on the
508 proportion of immune cells were gathered on mice that were euthanized at specific days post-
509 infection. Nevertheless, we could correlate the $CD4^+/CD8^+$ ratio at day 14 and 21 p.i. with the mortality
510 rate (the proportion of mice reaching the end points) within each experimental group and found that
511 indeed the higher the ratio the higher the mortality risk (spearman correlation, Rs = 0.766, n = 100, p
512 < 0.0001, fig. 15).

513 **Discussion**

514 We showed that the order of infection plays a paramount role in determining the outcome of
515 the coinfection between an intestinal nematode and a *Plasmodium* parasite. In particular, Py virulence
516 substantially increased when infecting hosts that were previously (or simultaneously) infected with Hp,
517 compared both to hosts with single infections and to hosts that were infected with Py first and then
518 with Hp. Contrary to Py, virulence of Hp was minimally affected by the coinfection, since Hp only
519 produced mild symptoms whatever the order of the infection. These results are partially in agreement
520 with our initial predictions. We hypothesized that previous infection with either Py or Hp would
521 polarize the immune response towards Th1 or Th2 effectors making the ground more favorable for a
522 subsequent infection, and resulting in more severe disease symptoms. This prediction was met when
523 Py infected mice harboring Hp, but not when Hp infected mice harboring Py. Therefore, there is a
524 strong asymmetry in the effect of coinfection between Py and Hp, depending on the order of the
525 infection. The increase in Py virulence in mice previously infected with Hp is consistent with previous
526 results on this system (Tetsutani et al. 2009), suggesting that previous Hp infection impairs the
527 subsequent immune response to Py (Noland et al. 2008; Tetsutani et al. 2009).

528 The possible evolutionary reasons underlying this asymmetry are manifold. Intestinal
529 nematodes usually produce chronic infections where the hosts keep shedding parasite eggs for months
530 or even years depending on the species (Morand 1996). Inter-host transmission success and parasite
531 fitness is tightly associated with the duration of egg shedding (patent period), therefore any parasite
532 trait that compromises host health and survival is likely counter selected in these systems. In
533 agreement with this view, nematode infections are usually well tolerated and host damage is usually
534 observed only when parasite burden is high (Brooker 2010; Lippens et al. 2016). Since reinfection was
535 not possible in our experiment, parasite burden was constrained by the initial number of infective
536 larvae given to the host. It might be interesting to investigate to what extent the lack of increase in Hp
537 virulence in coinfected hosts could change when using higher infective doses (Lippens et al. 2016), or
538 allowing hosts to be reinfected. Although the transmission success of Py cannot be directly assessed

539 from the proportion of iRBC, longer persistence of high parasite density, as observed in coinfected
540 hosts, should increase the likelihood of gametocyte production, as reported for other *Plasmodium*
541 species (see Tadesse et al. 2017). In agreement with this view, Py transmission success to the dipteran
542 vector was enhanced when mice were coinfected with the helminth *Echinostoma caproni* (Noland et
543 al. 2007). Therefore, the cost of virulence is probably higher in Hp than in Py. Alternatively, increased
544 Py virulence might be maladaptive if host overexploitation and death jeopardize parasite fitness
545 through reduced transmission success.

546 Whatever the benefit or disadvantage of changes in virulence for Py, from the host
547 perspective, coinfection did incur costs both in terms of general health and specific markers of Py
548 infection. In particular, whether single infected hosts still gained mass during the 5 weeks p.i., at a rate
549 that was similar to the non-infected hosts, coinfection induced a loss of body mass (when Py infected
550 mice previously infected with Hp) or temporarily slowed down the gain in body mass (when Hp infected
551 mice previously infected with Py). In agreement with the results on changes in body mass, host
552 mortality (reaching of the end points) was only reported in coinfection groups where Py followed the
553 Hp infection. Interestingly, there was no difference according to the timing of the infection, suggesting
554 that the importance of the order of the infection is conserved and relatively consistent over different
555 coinfection scenarios. In another coinfection model, involving the cestode *Taenia crassiceps* and
556 *Plasmodium yoelii* 17XL, Salazar-Castañón et al. (2018) found that coinfected mice had relatively longer
557 survival time compared to single Py infected hosts and that the gain in survival was related to the
558 timing of the infection (the longer the delay between the infection, the better the gain in survival time),
559 suggesting that the effect of timing of infection might be model-dependent.

560 Our prediction of increased virulence in coinfected hosts was based on the rationale that
561 previous infection with nematodes polarizes the immune system towards a Th2 response (Reynolds et
562 al. 2012). In agreement with this hypothesis, we found that Th2 indeed discriminated the three
563 experimental groups, with higher percentage of GATA-3^{+} within CD4^{+} T cells in coinfected hosts (when
564 Py follows Hp) compared to both single Py infected and non-infected mice. Accordingly, we also

565 predicted that coinfected mice should have an impaired capacity to deal with the Py infection and
566 indeed we found that parasitemia was still high at day 21 p.i. in coinfected hosts compared to single
567 Py infected mice. Therefore, direct damage produced by Py multiplication might account for the more
568 severe disease symptoms observed in coinfected hosts. In agreement with this view, changes in RBC
569 counts over the course of the infection mirrored changes in parasitemia, with coinfected groups still
570 suffering from anemia at day 21 p.i., when single Py infected mice had already started to recover.

571 The fitness consequences of the damage caused by Py multiplication also depend on the host
572 capacity to repair damaged tissues, or in other terms on the capacity to tolerate the infection
573 (Medzhitov et al. 2012). In particular, RBCs are constantly renewed during hematopoiesis and
574 therefore hosts that can restore lost RBCs at a faster pace should be able to better tolerate the
575 infection (i.e., to pay a smaller infection cost) compared to hosts with a slower rate of RBC renewal
576 (Chang et al. 2004). Given that coinfected hosts suffered from higher anemia, compensating for the
577 higher rate of RBC loss would have needed a higher production of reticulocytes. However, we found
578 that coinfected hosts had similar plasma levels of EPO and similar proportions of reticulocytes, as
579 assessed by the MGV, compared to single infected hosts. Therefore, despite higher parasitemia and
580 higher anemia, coinfected hosts only replaced RBCs at a similar rate of single infected hosts, and
581 therefore were less tolerant to the Py infection. This finding suggests that any improvement of the
582 capacity to renew lost RBCs should reduce the cost of coinfection. Indeed, experimental administration
583 of rEPO to coinfected hosts partially improved the symptoms of the disease, as also previously reported
584 (Kaiser et al. 2006), and improved host tolerance to the infection. However, the magnitude of the
585 effects was small, suggesting that other aspects of the physiopathology of the coinfection are probably
586 more important determinants of the coinfection costs. In addition, the production of reticulocytes also
587 replenishes the reservoir of cells that can be exploited by Py for its own replication, which can also
588 contribute to maintain parasitemia over longer period of time and possibly exacerbates disease
589 severity (Chang et al. 2004; Tsubata et al. 2005).

590 Massive release of free heme groups has the potential to damage host tissues through their
591 prooxidant, proinflammatory and cytotoxic effects (Kumar and Bandyopadhyay 2005; Immenschuh et
592 al. 2017). Previous studies have shown that the effectiveness of the mechanisms of detoxification of
593 free heme groups are key determinants of host survival (Pamplona et al. 2007; Seixas et al. 2009) and
594 liver function restoring once the parasite has been cleared (Dey et al. 2014), although the anti-
595 inflammatory properties of HO-1 might also promote liver infection (Epiphanio et al. 2008). We
596 therefore assessed the expression of the *Hmox1* gene in splenocytes and the amount of the enzyme
597 HO-1 in plasma. As for the renewal of lost RBCs, given that coinfected hosts had higher amount of free
598 hemoglobin compared to single infection (due to the higher RBC lysis), we expected to find a higher
599 expression of *Hmox1* and more HO-1 in plasma of coinfected hosts. However, although the gene was
600 overexpressed in coinfected mice (the gene was highly overexpressed in infected mice compared to
601 non-infected hosts), the amount of enzyme was similar in coinfected and single Py infected hosts,
602 possibly due to the degradation of the enzyme through the ubiquitin-proteasome system (Lin et al.
603 2008; Chau 2015). We also found that another mechanism allowing the host to deal with free
604 hemoglobin (the scavenger receptor CD163) (Kristiansen et al. 2001) was downregulated in RPM of
605 coinfected and single infected hosts.

606 Free heme group is also recognized as a DAMP by the immune system and can induce an
607 overreacting inflammatory response leading to host damage (Fortes et al. 2012). Coinfection between
608 Hp and another model species of murine malaria (*Plasmodium chabaudi* AS) has been reported to
609 increase host mortality (Su et al. 2005), due to liver pathology involving hepatic IFN-γ, IL-17 and IL-22
610 (Helmby 2009). Although infected hosts overexpressed IFN-γ, IL-10 and TGF-β1 compared to non-
611 infected mice, there was no difference between coinfected and single Py infected mice. Similarly, we
612 did not find any difference in the percentage of FoxP3$^+$ within CD4$^+$ T cells between single Py infected
613 and coinfected mice; however, the percentage of CTLA-4$^+$ within FoxP3$^+$ CD4$^+$ T cells was higher in
614 coinfected mice compared to single Py infected hosts during the peak of the acute infection. Therefore,
615 although we did not find an expansion of Treg in Py infected mice (as previously shown, Tetsutani et

616 al. 2009), the immunosuppressive capacities of Treg were upregulated in single Py infected mice, and
617 even more so in coinfected hosts through the CTLA-4 immune checkpoint (see Kurup et al. 2017).
618 Therefore, coinfected mice appeared to have an upregulated immunosuppressive function, possibly
619 accounting for the failure to control Py multiplication.

620 We went a step further by identifying 20 immune cell populations in the spleen by spectral
621 flow cytometry using a 27-color panel. The results of the PCA clearly showed that the three
622 experimental groups clustered in different areas of the space defined by the first two components,
623 and especially so at day 14 and 21 p.i., with the single Py infection group lying in between the non-
624 infected and the coinfection groups. The cell population that best discriminated between single Py
625 infected and coinfected hosts was the $CD8^+$ T cells that got exhausted more in coinfected mice. Several
626 Py epitopes are recognized by $CD8^+$ T cells during the blood stage of the infection (Howland et al. 2015).
627 Moreover, previous work has shown that $CD8^+$ T cells play a role in the protective immunity against
628 blood-stage infection with Py (Imai et al. 2010), and chronic infection with the nematode *Litosomoides*
629 *sigmodontis* interferes with the anti-*Plasmodium* $CD8^+$ T cell response (Kolbaum et al. 2012). Infection
630 with Hp has also been shown to suppress $CD8^+$ T cells in mice subsequently infected with the protozoan
631 *Toxoplasma gondii* (Khan et al. 2008). Exhaustion of $CD8^+$ cells results from the overexpression of
632 immune checkpoints whose function is to avoid immunopathology during persistent antigenic
633 exposure (Chandele et al. 2010; Wykes and Lewin 2018; McLane et al. 2019). In agreement with this,
634 we found that the proportion of both PD-1^+ and LAG-3^+ within $CD8^+$ T cells was higher in coinfected
635 hosts compared to single Py infection at day 14 post-infection. Mechanisms supposed to protect the
636 hosts from immunopathology (Howland et al. 2015) might thus actually make them more susceptible
637 to parasite exploitation (Scholzen et al. 2009; Frimpong et al. 2019), and especially so when hosts are
638 coinfected by parasites with different exploitation strategies.

639 One of the consequences of the $CD8^+$ exhaustion is an increase of the ratio between $CD4^+$ and
640 $CD8^+$ T cells. Deviations of the $CD4^+/CD8^+$ ratio from the homeostatic values (inverted ratio below 1, or
641 increased values above 2.5) have been investigated in a few host-pathogen systems, and found to

642 correlate with poor host survival prospects (McBride and Striker 2017). For instance, high values of the
643 $CD4^+/CD8^+$ ratio have been shown to be predictors of patient mortality during SARS-CoV-2 infection
644 (De Zunai et al. 2021; Pascual-Dapena et al. 2022). We found similar results, although the correlation
645 between the $CD4^+/CD8^+$ ratio and mortality could only be assessed at the population (inter-group)
646 level. The increase of the $CD4^+/CD8^+$ ratio probably reflects a global, temporary, dysfunction of the
647 immune response, which favors the replication rate of Py in coinfected hosts. In agreement with this
648 view, BALB/c mice infected with Py and depleted of $CD8^+$ T cells suffered from greater parasitemia and
649 higher mortality compared to control individuals during the period of peak parasitemia (Imai et al.
650 2015).

651 This work provides some relevant findings for the epidemiology of the coinfection between
652 nematodes and *Plasmodium* and possibly for the evolution of virulence when parasites exploit the
653 same host. In terms of the epidemiology of the disease, a key question is whether infection order is
654 random or if it intrinsically depends on the life cycle of the parasite. We suggest that, in the specific
655 case of the coinfection between gastrointestinal nematodes and *Plasmodium*, hosts might have higher
656 chances to suffer from ordered infections where *Plasmodium* infects hosts already harboring worms.
657 This suggestion is based on the observation that gastrointestinal nematodes usually establish chronic,
658 steady state, infections that can last for months (or even years for some human helminths) while
659 *Plasmodium* produces acute infections (lasting 2-4 weeks) that can either be cleared or lead to
660 subsequent relapses (again depending on the parasite and the host species). However, this hypothesis
661 rests on the assumption that hosts have equal probabilities to be infected by the two parasites per unit
662 of time, or in other words that the probability of infection is not age-dependent. It should also be
663 reminded that our experimental work only considered primary infections (reinfection was not
664 allowed). However, in the real world, hosts are repeatedly exposed to multiple parasites and when
665 there is no sterilizing immunity, previous infection does not fully prevent subsequent reinfection. The
666 complexity due to age-dependent probability of infection and repeated exposure/infection might
667 therefore blur the importance of the infection order as a driver of disease severity.

We also think that these results are relevant to predict how selection might shape the optimal level of virulence (defined as infection-induced host damage) when parasites exploit hosts that harbor coinfecting parasites that elicit different immune effectors. A key prediction here is that species-specific cost of virulence might constraint the evolution of host damage in different ways in coinfecting parasites. Experimental evolution and theoretical modelling would be valuable tools to explore this question.

A final thought is that, although we considered that the coinfection dynamics with *Plasmodium* and nematodes is regulated by top-down mechanisms involving the host immune response, we cannot ignore that both parasites (and nematodes in particular) can also interfere with the host immune response for their own benefit. This paves the way for a scenario where the top-down mechanisms might also be under parasite control.

Acknowledgments

We are grateful to Valérie Saint Giorgio and all the staff of the animal facility for taking care of the animals.

Funding

The work has been funded by the French Agence Nationale de la Recherche (grant # ANR-21-CE35-0015).

Author contribution

GS, BF, MR and BR conceived the study and gathered the funding; AD, LB, NP, GS and BF collected the data; AD, LB, EG performed the lab work; NP assisted with the spectral flow cytometry analysis; GS analyzed the data; GS, AD and LB wrote the first draft of the manuscript; all authors revised and approved the final version.

Data availability statement

All the data will be made available in DRYAD once the manuscript has been accepted for publication.

694 **Conflict of interest**

695 The authors declare no conflict of interest.

696

697 **References**

698 Adegnika AA, Kremsner PG. 2012. Epidemiology of malaria and helminth interaction: e review from
699 2001 to 2011. Current Opinion in HIV and AIDS 7: 221-224.

700 Afolabi MO, Ale BM, Dabira ED, Agbla SC, Bustinduy AL, Ndiaye JLA, Greenwood B. 2021. Malaria and
701 helminth co-infections in children living in endemic countries: A systematic review with meta-
702 analysis. PLoS Neglected Tropical Diseases 15: e0009138.

703 Alizon S, de Roode JC, Michalakis Y. 2013. Multiple infections and the evolution of virulence. Ecology
704 Letters 16, 556-567.

705 Bansemir AD, Sukhdeo MVK. 1994. The food resource of adult *Heligmosomoides polygyrus* in the small
706 intestine. Journal of Parasitology 80, 24.

707 Billet LS, Wuerthner VP, Hua J, Relyea RA, Hoverman JT. 2020. Timing and order of exposure to two
708 echinostome species affect patterns of infection in larval amphibians. Parasitology 147: 1515-
709 1523.

710 Brooker S. 2010. Estimating the global distribution and disease burden of intestinal nematode
711 infections: Adding up the numbers – A review. International Journal for Parasitology 40: 1137-
712 1144.

713 Budischak SA, Wiria AE, Hamid F, Wammes LJ, Kaisar MMM, van Lieshout L, Sartono E, Supali T,
714 Yazdanbakhsh M, Graham AL. 2018. Competing for blood: the ecology of parasite resource
715 competition in human malaria-helminth co-infections. Ecology Letters 21: 536.

716 Chandele A, Mukerjee P, Das G, Ahmed R, Chauhan VS. Phenotypic and functional profiling of malaria-
717 induced CD8 and CD4 T cells during blood-stage infection with *Plasmodium yoelii*. Immunology
718 132: 273-286.

719 Chang K-H, Tam M, Stevenson MM. 2004. Modulation of the course and outcome of blood-stage
720 malaria by erythropoietin-induced reticulocytosis. The Journal of Infectious Diseases 189: 735-
721 743.
722 Chau L-Y. 2015. Heme oxygenase-1: emerging target of cancer therapy. Journal of Clinical Science 22:
723 22.
724 Clay PA, Rudolf VHW. 2019. How parasite interaction strategies alter virulence evolution in multi-
725 parasite communities. Evolution 73: 2189.
726 Coelho CH, Gazzinelli-Guimaraes PH, Howard J, Barnafo E, Alani NAH, Muratova O, McCormack A,
727 Kelnhofer E, Urban Jr JF, Narum DL, Anderson C, Langhorne J, Nutman TB, Duffy PE. 2019.
728 Chronic helminth infection does not impair immune response to malaria transmission blocking
729 vaccine Pfs230D1-EPA/Alhydrogel® in mice. Vaccine 37: 1038-1045.
730 Craig JM, Scott AL. 2017. Antecedent *Nippostrongylus* infection alters the lung immune response to
731 *Plasmodium berghei*. Parasite Immunology 39: e12441.
732 Degarege A, Erko B. 2016. Epidemiology of *Plasmodium* and helminth coinfection and possible reasons
733 for heterogeneity. BioMed Research International 2016: 3083568.
734 Degarege A, Veledar E, Degarege D, Erko B, Nacher M, Madhivanan P. 2016. *Plasmodium falciparum*
735 and soil-transmitted helminth co-infections among children in sub-Saharan Africa: a systematic
736 review and meta-analysis. Parasite Vectors 9: 344.
737 Dey S, Mazumder S, Siddiqui AA, Iqbal MS, Banerjee C, Sarkar S, De R, Goyal M, Bindu S,
738 Bandyopadhyay U. 2014. Association of heme oxygenase 1 with the restoration of liver function
739 after damage in murine malaria by *Plasmodium yoelii*. Infection and Immunity 8: 3113-3126.
740 De Zuani M, Laznickova P, Tomaskova V, Dvoncovan M, Forte G, Stokin GB, Sramek V, Helan M, Fric J.
741 2022. High CD4-to-CD8 ratio identifies an at-risk population susceptible to lethal COVID-19.
742 Scandinavian Journal of Immunology 95: e13125.
743 Epiphanio S, Mikolajczak SA, Gonçalves LA, Pamplona A, Portugal S, Albuquerque S, Goldberg M,
744 Rebelo S, Anderson DG, Akinc A, Vomlocher H-P, Kappe SHI, Soares MP, Mota MM. Heme

745 oxygenase-1 is an anti-inflammatory host factor that promotes murine *Plasmodium* liver
746 infection. Cell Host & Microbe 3: 331-338.
747 Ezenwa VO, Jolles AE. 2011. From host immunity to pathogen invasion: the effects of helminth
748 coinfection on the dynamics of microparasites. Integrative and Comparative Biology 51: 540.
749 Fenton A. 2013. Dances with worms: the ecological and evolutionary impacts of deworming on
750 coinfecting pathogens. Parasitology 140: 1119-1132.
751 Filbey KJ, Camberis M, Chandler J, Turner R, Kettle AJ, Eichenberger RM, Giacomin P, Le Gros G. 2019.
752 Intestinal helminth infection promotes IL-5- and $CD4^+$ T cell-dependent immunity in the lung
753 against migrating parasites. Mucosal Immunology 12: 352-362.
754 Fortes GB, Alves LS, de Oliveira R, Dutra FF, Rodrigues D, Fernandez PL, Souto-Padron, T, De Rosa MJ,
755 Kelliher M, Golenbock D, Chan FKM, Bozza MT. 2012. Heme induces programmed necrosis on
756 macrophages through autocrine TNF and ROS production. Blood 119: 2368-2375.
757 Frimpong A, Kusi KA, Adu-Gyasi D, Amponsah J, Ofori MF, Ndifon W. 2019. Phenotypic evidence of T
758 cell exhaustion and senescence during symptomatic *Plasmodium falciparum* malaria. Frontiers
759 in Immunology 10: 1345.
760 Graham AL. 2008. Ecological rules governing helminth-microparasite coinfection. PNAS 105: 566.
761 Gregory RD Montgomery SSJ, Montgomery WI. 1992. Population biology of *Heligmosomoides*
762 *polygyrus* (Nematoda) in the wood mouse. Journal of Animal Ecology 61: 749-757.
763 Griffiths EC, Fairlie-Clarke K, Allen JE, Metcalf CJE, Graham AL. 2015. Bottom-up regulation of malaria
764 population dynamics in mice co-infected with lung-migratory nematodes. Ecology Letters 18:
765 1387-1396.
766 Hartgers FC, Yazdanbakhsh M. 2006. Co-infection of helminths and malaria: modulation of the immune
767 responses to malaria. Parasite Immunology 28: 497.
768 Helmby H. 2009. Gastrointestinal nematode infection exacerbates malaria-induced liver pathology.
769 Journal of Immunology 182: 5663.

770 Howland SW, Claser C, Poh CM, Gun SY, Rénia L. 2015. Pathogenic CD8$^+$ T cells in experimental cerebral
771 malaria. Seminars in Immunopathology 37: 221-231.
772 Hürlimann E, Houngbedji CA, Yapi RB, N'Dri PB, Silué KD, Ouattara M, Utzinger J, N'Goran EK, Raso G.
773 2019. Antagonistic effects of *Plasmodium*-helminth co-infection on malaria pathology in
774 different population groups in Côte d'Ivoire. PLoS Neglected Tropical Diseases 13: e0007086.
775 Imai T, Shen J, Chou B, Duan X, Tu L, Tetsutani K, Moriya C, Ishida H, Hamano S, Shimokawa C, Hisaeda
776 H, Himeno K. 2010. Involvement of CD8$^+$ T cells in protective immunity against murine blood-
777 stage infection with *Plasmodium yoelii* 17XL strain. European Journal of Immunology 40: 1053-
778 1061.
779 Imai T, Ishida H, Suzue K, Taniguchi T, Okada H, Shimokawa C, Hisaeda H. 2015. Cytotoxic activities of
780 CD8$^+$ T cells collaborate with macrophages to protect against blood-stage murine malaria. eLIFE
781 4: e04232.
782 Imrie R, Walsh SK, Roberts KE, Lello J, Longdon B. 2023. Investigating the outcomes of virus coinfection
783 within and across host species. PLoS Pathogens 19: e1011044.
784 Immenschuh S, Vijayan V, Janciauskiene S, Gueler F. 2017. Heme as a target for therapeutic
785 interventions. Frontiers in Pharmacology 8: 146.
786 Kaiser K, Texier A, Ferrandiz J, Meiller A, Latour C, Peyron F, Cespuglio R, Picot S. 2006. Recombinant
787 human erythropoietin prevents the death of mice during cerebral malaria. Journal of Infectious
788 Diseases 193: 987-995.
789 Karvonen A, Jokela J, Laine A-L. 2019. Importance of sequence and timing in parasite coinfections.
790 Trends in Parasitology 35: 109-118.
791 Khan IA, Hakak R, Eberle K, Sayles P, Weiss LM, Urban Jr JF. 2008. Coinfection with *Heligmosomoides*
792 *polygyrus* fails to establish CD8$^+$ T-cell immunity against *Toxoplasma gondii*. Infection and
793 Immunity 76: 1305-1313.
794 Knowles SCL. 2011. The effect of helminth co-infection on malaria in mice: a meta-analysis.
795 International Journal for Parasitology 41: 1041.

796 Kolbaum J, Escbach M-L, Steeg C, Jacobs T, Fleischer B, Breloer M. 2012. Efficient control of
797 *Plasmodium yoelii* infection in BALB/c and C57BL/6 mice with pre-existing *Strongyloides ratti*
798 infection. Parasite Immunology 34: 388-393.
799 Kolbaum J, Tartz S, Hartmann W, Helm S, Nagel A, Heussler V, Sebo P, Fleischer B, Jacobs T, Breloer M.
800 2012. Nematode-induced interference with the anti-Plasmodium $CD8^+$ T-cell response can be
801 overcome by optimizing antigen administration. European Journal of Immunology 42: 890-900.
802 Kotepui M, Mala W, Kwankaew P, Kotepui KU, Ramirez Masangkay F, Wilairatana P. 2023. Distinct
803 cytokine profiles in malaria coinfection: A systematic review. PLoS Neglected Tropical Diseases
804 17: e0011061.
805 Kristiansen M, Graversen JH, Jacobsen C, Sonne O, Hoffman HJ, Law SK, Moestrup SK. 2001.
806 Identification of the haemoglobin scavenger receptor. Nature 409: 198-201.
807 Kumar S, Bandyopadhyay U. 2005. Free heme toxicity and its detoxification systems in human.
808 Toxicology Letters 157: 175-188.
809 Kurup SP, Obeng-Adjei N, Anthony SM, Traore B, Doumbo OK, Butler NS, Crompton PD, Harty JT. 2017.
810 Regulatory T cells impede acute and long-term immunity to blood-stage malaria through CTLA-
811 4. Nature Medicine 23: 1220-1227.
812 Kwan JL, Seitz AE, Fried M, Lee K-L, Metenou S, Morrison R, Kabyemela E, Nutman TB, Prevots DR,
813 Duffy PE. 2018. Seroepidemiology of helminths and the associations with severe malaria among
814 infants and young children in Tanzania. PLoS Neglected Tropical Diseases 12: e0006345.
815 Lin P-H, Chiang M-T, Chau L-Y. 2008. Ubiquitin-proteasome system mediates heme oxygenase-1
816 degradation through endoplasmatic reticulum-associated degradation pathway. Biochimica et
817 Biophysica Acta 1783: 1826-1834.
818 Lippens C, Guivier E, Faivre B, Sorci G. 2016. Reaction norms of host immunity, host fitness and parasite
819 performance in a mouse - intestinal nematode interaction. International Journal for Parasitology
820 46: 133-140.

821 Ma Y, Su X-Z, Lu F. 2020. The roles of Type I interferon in co-infections with parasites and viruses,
822 bacteria, or other parasites. Frontiers in Immunology 11: 1805.
823 McBride JA, Striker R. 2017. Imbalance in the game of T cells: What can the CD4/CD8 T-cell ratio tell us
824 about HIV and health? PLoS Pathogens 13: e1006624.
825 McLane, L, Abdel-Hakeem MS, Wherry EJ. 2019. CD8 T cell exhaustion during chronic viral infection
826 and cancer. Annual Review of Immunology 37: 457-495.
827 Medzhitov R, Schneider DS, Soares MP. 2012. Disease tolerance as a defense strategy. Science 335:
828 936-941.
829 Morand S. 1996. Life-history traits in parasitic nematodes: a comparative approach for the search of
830 invariants. Functional Ecology 10: 210-218.
831 Nacher M. 2011. Interactions between worms and malaria: good worms or bad worms? Malaria
832 Journal 10: 259.
833 Noland GS, Chowdhury DR, Urban Jr JF, Zavala F, Kumar N. 2010. Helminth infection impairs the
834 immunogenicity of a *Plasmodium falciparum* DNA vaccine, but not irradiated sporozoites, in
835 mice. Vaccine 28: 2917-2923.
836 Noland GS, Graczyk TK, Fried B, Kumar N. 2007. Enhanced malaria parasite transmission from helminth
837 co-infected mice. American Journal of Tropical Medicine and hygiene 76: 1052.
838 Noland GS, Urban JF, Fried B, Kumar N. 2008. Counter-regulatory anti-parasite cytokine responses
839 during concurrent *Plasmodium yoelii* and intestinal helminth infections in mice. Experimental
840 Parasitology 119: 272-278.
841 Olatunde AC, Cornwall DH, Roedel M, Lamb TJ. 2022. Mouse models for unravelling immunology of
842 blood stage malaria. Vaccines 10: 1525.
843 Paludan SR. 1998. Interleukin-4 and interferon-γ: the quintessence of a mutual antagonistic
844 relationship. Scandinavian Journal of Immunology 48: 459-468.
845 Pamplona A, Ferreira A, Balla J, Jeney V, Balla G, Epiphanio S, Chora A, Rodrigues CD, Gregoire IP,
846 Cunha-Rodrigues M, Portugal S, Soares MP, Mota MM. 2007. Heme oxygenase-1 and carbon

847 monoxide suppress the pathogenesis of experimental cerebral malaria. Nature Medicine 13:
848 703–710.
849 Pascual-Dapena A, Chillaron JJ, Llauradó G, Arnau-Barres I, Flores J, Lopez-Montesinos I, Sorlí L,
850 Martinez-Pérez JL, Gómez-Zorrilla S, Du J, García-Giralt N, Güerri-Fernández R. 2022. Individuals
851 with higher CD4/CD8 ratio exhibit increased risk of acute respiratory distress syndrome and in-
852 hospital mortality during acute SARS-CoV-2 infection. Frontiers in Medicine 9: 924267.
853 Reynolds LA, Filbey KJ, Maizels RM. 2012. Immunity to the model intestinal helminth parasite
854 *Heligmosomoides polygyrus*. Seminars in Immunopathology 34: 829-846.
855 Salazar-Castañón VH, Juárez-Avelar I, Legorreta-Herrera M, Govezensky T, Rodriguez-Sosa M. 2018.
856 Co-infection: the outcome of *Plasmodium* infection differs according to the time of pre-existing
857 helminth infection. Parasitology Research 117: 2767.
858 Salazar-Castañón VH, Legorreta-Herrera M, Rodriguez-Sosa M. 2014. Helminth parasites alter
859 protection against *Plasmodium* infection. BioMed Research International 2014: 913696.
860 Scholzen A, Minigo G, Plebanski M. 2009. Heroes or villains? T regulatory cells in malaria infection.
861 Trends in Parasitology 26: 16-25.
862 Seixas E, Gozzelino R, Chora A, Ferreira A, Silva G, Larsen R, Rebelo S, Penido C, Smith NR, Coutinho A,
863 Soares MP. 2009. Heme oxygenase-1 affords protection against noncerebral forms of severe
864 malaria. Proceedings of the National Academy of Sciences 106: 15837-15842.
865 Segura M, Matte C, Thawani N, Su Z, Stevenson MM. 2009. Modulation of malaria-induced
866 immunopathology by concurrent gastrointestinal nematode infection in mice. International
867 Journal for Parasitology 39: 1525.
868 Shen S-S, Qu X-Y, Zhang W-Z, Li J, Lv Z-Y. 2019. Infection against infection: parasite antagonism against
869 parasites, viruses and bacteria. Infectious Diseases of Poverty 8: 49.
870 Su Z, Segura M, Morgan K, Loredo-Osti JC, Stevenson MM. 2005. Impairment of protective immunity
871 to blood-stage malaria by concurrent nematode infection. Infection and Immunity 73: 3531-
872 3539.

873 Su Z, Segura M, Stevenson MM. 2006. Reduced protective efficacy of a blood-stage malaria vaccine by
874 concurrent nematode infection. Infection and Immunity 74: 2138-2144.
875 Supali T, Verweij JJ, Wiria AE, Djuardi Y, Hamid F, Kaisar MMM, Wammes LJ, van Lieshout L, Luty AJF,
876 Sartoro E, Yazdanbakhsh M. 2010. Polyparasitism and its impact on the immune system.
877 International Journal for Parasitology 40: 1171-1176.
878 Szabo E, Bowhay C, Forrester E, Liu H, Dong B, Coria AL, Perera S, Fung B, Badawadagi N, Gaio C, Bailey
879 K, Ritz M, Bowron J, Ariyaratne A, Finney CAM. 2024. *Heligmosomoides bakeri* and *Toxoplasma*
880 *gondii* co-infection leads to increased mortality associated with changes in immune resistance
881 in the lymphoid compartment and disease pathology. PLoS ONE 19: e02922408.
882 Tadesse FG, van den Hoogen L, Lanke K, Schildkraut J, Tetteh K, Aseffa A, Mamo H, Sauerwein R, Felger
883 I, Drakeley C, Gadissa E, Bousema T. 2017. The shape of the iceberg: quantification of
884 submicroscopic *Plasmodium falciparum* and *Plasmodium vivax* parasitemia and gametocytemia
885 in five low endemic settings in Ethiopia. Malaria Journal 16: 99.
886 Tetsutani K, Ishiwata K, Ishida H, Tu L, Torii M, Hamano S, Himeno K, Hisaeda H. 2009. Concurrent
887 infection with *Heligmosomoides polygyrus* suppresses anti-*Plasmodium yoelii* protection
888 partially by induction of $CD4^{+}CD25^{+}Foxp3^{+}$ Treg in mice. European Journal of Immunology 39:
889 2822-2830.
890 Tsubata S, Ebe K, Kawamura T, Ishimoto Y, Tomiyama-Miyaji C, Watanabe H, Sekikawa H, Aoyagi Y,
891 Abo T. 2005. Protection against malaria by anti-erythropoietin antibody due to suppression of
892 erythropoiesis in the liver and at other sites. Immunology and Cell Biology 83: 638-642.
893 Viney ME, Graham AL. 2013. Patterns and processes in parasite co-infection. Advances in Parasitology
894 82: 321-369.
895 Wait LF, Kamiya T, Fairlie-Clarke KJ, Metcalf CJE, Graham AL, Mideo N. 2021. Differential drivers of
896 intraspecific and interspecific competition during malaria-helminth co-infection. Parasitology
897 148: 1030-1039.

898 Webb EL, Ekii AO, Pala P. 2012. Epidemiology and immunology of helminth-HIV interactions. Current
899 Opinion in HIV and AIDS 7: 245-253.
900 Wykes MN, Lewin SR. 2018. Immune checkpoint blockade in infectious diseases. Nature Reviews
901 Immunology 18: 91-104.
902
903
904

905 Table 1. General linear mixed model investigating the changes in body mass (percent variation with
906 respect to day 0) in non-infected and single (Hp and Py) infected mice. We report the parameter
907 estimates with the 95% CI, degrees of freedom (df), F and p values. Mouse ID was included as a random
908 effect to take into account the non-independence of observations for the same individual over time.
909 N = 120 individuals and 774 observations.

Fixed effects		**Estimate**	**95% CI**	**df**	**F**	**p**
Treatment				2,648	0.24	0.7828
	Non-infected	0				
	Hp	-0.47	-3.13/2.20			
	Py	-0.95	-3.60/1.71			
Time		0.54	0.35/0.74	1,648	83.44	<0.0001
Squared time		-0.004	-0.01/0.001	1,648	2.80	0.095
Time*Treatment				2,648	0.12	0.8827
	Non-infected	0				
	Hp	0.007	-0.27/0.29			
	Py	-0.06	-0.33/0.22			
Squared Time*Treatment				2,648	0.88	0.4141
	Non-infected	0				
	Hp	0.0003	-0.01/0.01			
	Py	0.005	-0.003/0.01			
Random effect		**Estimate**	**SE**	**z**	**P**	
ID		16.49	2.49	6.62	<0.0001	

910

911

912 Table 2. General linear mixed model investigating the changes in body mass (percent variation with
913 respect to day 0) in non-infected, single Py infected and coinfected (Hp infecting first and simultaneous
914 infection) mice. We report the parameter estimates with the 95% CI, degrees of freedom (df), F and p
915 values. Mouse ID was included as a random effect to take into account the non-independence of
916 observations for the same individual over time. N = 196 individuals and 1009 observations.

Fixed effects		**Estimate**	**95% CI**	**df**	**F**	**P**
Infection				2,807	3.0	0.0503
	Non-infected	0				
	Single	-4.50	-8.2/-0.8			
	Coinfection	-1.55	-4.6/1.5			
Time		0.60	0.14/1.06	1,807	76.87	<0.0001
Squared time		-0.01	-0.03/0.01	1,807	56.88	<0.0001
Time*Infection				2,807	3.57	0.0285
	Non-infected	0				
	Single	0.88	0.23/1.53			
	Coinfection	0.47	-0.07/1.01			
Squared Time*Infection				2,807	9.72	<0.0001
	Non-infected	0				
	Single	-0.04	-0.07/-0.01			
	Coinfection	-0.05	-0.07/-0.03			
Random effect		**Estimate**	**SE**	**Z**	**p**	
ID		16.7	2.1	7.95	<0.0001	

917

918

Table 3. General linear mixed model investigating the changes in body mass (percent variation with respect to day 0) in non-infected, single Hp infected and coinfected (Py infecting first) mice. We report the parameter estimates with the 95% CI, degreed of freedom (df), F and p values. Mouse ID was included as a random effect to take into account the non-independence of observations for the same individual over time. N = 155 individuals and 869 observations.

Fixed effects		**Estimate**	**95% CI**	**df**	**F**	**p**
Infection				2,708	1.06	0.3477
	Non-infected	0				
	Single	-0.52	-2.61/1.57			
	Coinfection	0.8	-1.042.64			
Time		0.54	0.40/0.68	1,708	86.46	<0.0001
Squared time		-0.004	-0.008/-0.0005	1,708	0.58	0.4468
Time*Infection				2,708	22.19	<0.0001
	Non-infected	0				
	Single	0.007	-0.2/0.21			
	Coinfection	-0.52	-0.70/-0.34			
Squared Time*Infection				2,708	9.50	<0.0001
	Non-infected	0				
	Single	0.0007	-0.005/0.006			
	Coinfection	0.01	0.005/0.015			
Random effect		**Estimate**	**SE**	**z**	**P**	
ID		11.96	1.62	7.37	<0.0001	

926 Table 4. General linear mixed model investigating the changes in parasitemia (proportion of iRBC) in
927 single Py infection and coinfected (Hp infecting first and simultaneous infection). We report the
928 parameter estimates with the 95% CI, degrees of freedom (df), F and p values. Mouse ID was included
929 as a random effect to take into account the non-independence of observations for the same individual
930 over time. The distribution of errors was modelled using a beta distribution. N = 151 individuals and
931 665 observations.

Fixed effects		**Estimate**	**95% CI**	**df**	**F**	**p**
Infection				1,510	11.3	0.0008
	Single	0				
	Coinfection	1.95	0.81/3.1			
Time		1.05	0.9/1.2	1,510	428.25	<0.0001
Squared time		-0.03	-0.04/0.02	1,510	230.38	<0.0001
Time*Infection				1,510	12.12	0.0005
	Single	0				
	Coinfection	-0.3	-0.48/-0.13			
Squared Time*Infection				1,510	17.63	<0.0001
	Single	0				
	Coinfection	0.01	0.007/0.019			
Random effect		**Estimate**	**SE**	**z**	**p**	
ID		0.139	0.032	4.32	<0.0001	

932

933

934 Table 5. General linear mixed model investigating the changes in RBC counts (10^6/µl) in non-infected
935 and single (Hp, Py) infected mice. We report the parameter estimates with the 95% CI, degrees of
936 freedom (df), F and p values. Mouse ID was included as a random effect to take into account the non-
937 independence of observations for the same individual over time. N = 60 individuals and 360
938 observations.

Fixed effects		**Estimate**	**95% CI**	**df**	**F**	**p**
Treatment				2,291	5.27	0.0056
	Non-infected	0				
	Hp	0.709	0.101/1.361			
	Py	0.967	0.36/1.574			
Time		-0.224	-0.35/-0.098	1,291	197.56	<0.0001
Squared time		0.013	0.003/0.023	1,291	86.17	<0.0001
Cubic time		-0.0002	-0.0004/-5^{e-6}	1,291	39.83	<0.0001
Time*Treatment				2,291	36.27	<0.0001
	Non-infected	0				
	Hp	-0.163	-0.344/0.017			
	Py	-0.735	-0.913/-0.557			
Squared time*Treatment				2,291	9.55	<0.0001
	Non-infected	0				
	Hp	0.011	-0.003/0.025			
	Py	0.031	0.017/0.045			
Cubic time*Treatment				2,291	2.22	0.1101
	Non-infected	0				
	Hp	-0.0002	-0.0005/0.00008			
	Py	-0.0003	-0.0006/-0.00001			
Random effect		**Estimate**	**SE**	**z**	**P**	
ID		0.1415	0.061	2.37	0.0089	

939

940

941 Table 6. General linear mixed model investigating the changes in RBC count (10^6/µl) in non-infected,
942 single Py infected and coinfected (Hp infecting first and simultaneous infection) mice. We report the
943 parameter estimates with the 95% CI, degreed of freedom (df), F and p values. Mouse ID was included
944 as a random effect to take into account the non-independence of observations for the same individual
945 over time. N = 94 individuals and 476 observations.

Fixed effects		**Estimate**	**95% CI**	**df**	**F**	**p**
Infection				2,373	1.70	0.1840
	Non-infected	0				
	Single	0.263	-0.40/0.92			
	Coinfected	-0.24	-0.79/0.31			
Time		-0.074	-0.29/0.14	1,373	0.03	0.8556
Squared time		-0.006	-0.032/0.021	1,373	67.42	<0.0001
Cubic time		0.0004	-0.0004/0.001	1,373	108.37	<0.0001
Time*Infection				2,373	0.73	0.4826
	Non-infected	0				
	Single	0.166	-0.14/0.471			
	Coinfected	0.024	-0.23/0.28			
Squared Time*Infection				2,373	11.62	<0.0001
	Non-infected	0				
	Single	-0.09	-0.127/-0.052			
	Coinfected	-0.057	-0.088/-0.026			
Cubic Time*Infection				2,373	17.96	<0.0001
	Non-infected	0				
	Single	0.004	0.002/0.005			
	Coinfected	0.002	0.001/0.003			
Random effect		**Estimate**	**SE**	**z**	**P**	
ID		0.37	0.084	4.37	<0.0001	

946

947

Table 7. General linear mixed model investigating the changes in mean globular volume (fL) in non-infected and single (Hp, Py) infected mice. We report the parameter estimates with the 95% CI, degrees of freedom (df), F and p values. Mouse ID was included as a random effect to take into account the non-independence of observations for the same individual over time. N = 60 individuals and 360 observations.

Fixed effects		**Estimate**	**95% CI**	**df**	**F**	**p**
Treatment				2,291	1.90	0.151
	Non-infected	0				
	Hp	0.658	-2.108/3.424			
	Py	-1.975	-4.738/0.789			
Time		0.486	-0.09/1.061	1,291	8.14	0.0046
Squared time		-0.026	-0.071/0.02	1,291	0.94	0.3326
Cubic time		0.0003	-0.0006/0.001	1,291	8.0	0.005
Time*Treatment				2,291	3.20	0.0423
	Non-infected	0				
	Hp	-0.529	-1.354/0.295			
	Py	0.53	-0.284/1.343			
Squared Time*Treatment				2,291	3.37	0.0358
	Non-infected	0				
	Hp	0.032	-0.033/0.097			
	Py	0.084	0.02/0.148			
Cubic Time*Treatment				2,291	10.55	<0.0001
	Non-infected					
	Hp	-0.0005	-0.002/0.0008			
	Py	-0.003	-0.004/-0.002			
Random effect		**Estimate**	**SE**	**z**	**P**	
ID		2.86	1.18	2.42	0.0078	

Table 8. General linear mixed model investigating the changes in mean globular volume (fL) in non-infected, single Py infected and coinfected (Hp infecting first and simultaneous infection) mice. We report the parameter estimates with the 95% CI, degrees of freedom (df), F and p values. Mouse ID was included as a random effect to take into account the non-independence of observations for the same individual over time. N = 94 individuals and 476 observations.

Fixed effects		**Estimate**	**95% CI**	**df**	**F**	**P**
Infection				2,373	1.05	0.3518
	Non-infected	0				
	Single	2.1	-1.05/5.25			
	Coinfection	1.7	-0.91/4.31			
Time		0.6	-0.54/1.75	1,373	45.87	<0.0001
Squared time		-0.04	-0.18/0.1	1,373	111.07	<0.0001
Cubic time		0.0008	-0.004/0.005		109.01	
Time*Infection				2,373	17.09	<0.0001
	Non-infected	0				
	Single	-4.36	-5.98/-2.73			
	Coinfection	-3.56	-4.92/-2.21			
Squared Time*Infection				2,373	30.02	<0.0001
	Non-infected	0				
	Single	0.71	0.51/0.90			
	Coinfection	0.58	0.41/0.74			
Cubic Time*Infection				2,373	27.42	<0.0001
	Non-infected	0				
	Single	-0.02	-0.03/0.016			
	Coinfection	-0.02	-0.02/0.012			
Random effect		**Estimate**	**SE**	**z**	**p**	
ID		4.28	1.25	3.44	0.0003	

962 Table 9. General linear mixed model investigating the relationship between RBC counts (log 10^6/µl)
963 and parasitemia (log proportion iRBC) in single Py infected and coinfected (Hp infecting first and
964 simultaneous infection) mice. We report the parameter estimates with the 95% CI, degrees of freedom
965 (df), F and p values. Mouse ID was included as a random effect to take into account the non-
966 independence of observations for the same individual over time. N = 48 individuals and 298
967 observations.

Fixed effects		**Estimate**	**95% CI**	**df**	**F**	**P**
Infection				1,248	8.71	0.0035
	Single	0				
	Coinfection	-0.199	-0.331/-0.066			
Parasitemia		-0.300	-0.341/-0.259	1,248	646.17	<0.0001
Infection*Parasitemia				1,248	9.14	0.0028
	Single	0				
	Coinfection	-0.081	-0.134/-0.028			
Random effect		**Estimate**	**SE**	**z**	**p**	
Mouse ID		0.015	0.006	2.51	0.0061	

968

969

970 Table 10. General linear mixed model investigating the changes in body mass (g) in coinfected (Hp-
971 28+Py) mice treated or not treated with rEPO. We report the parameter estimates with the 95% CI,
972 degrees of freedom (df), F and p values. Mouse ID was included as a random effect to take into account
973 the non-independence of observations for the same individual over time. N = 20 individuals and 245
974 observations.

Fixed effects		**Estimate**	**95% CI**	**df**	**F**	**P**
Treatment				1,221	0.27	0.6055
	Control	0				
	rEPO	-0.35	-1.67/0.98			
Time		0.2	0.11/0.29	1,221	31.59	<0.0001
Squared time		-0.012	-0.016/-0.008	1,221	40.36	<0.0001
Time*Treatment				1,221	0.75	0.3878
	Control	0				
	rEPO	-0.05	-0.18/0.069			
Squared Time*Treatment				1,221	6.78	0.0098
	Control	0				
	rEPO	0.007	0.002/0.013			
Random effect		**Estimate**	**SE**	**z**	**p**	
ID		1.77	0.61	2.91	0.0018	

975

976

977 Table 11. Generalized linear model with a beta distribution of errors investigating the changes in the
978 proportion of CTLA-4$^+$ within FoxP3$^+$ CD4$^+$ T cells in non-infected, single Py infected and coinfected (Hp
979 infecting first and simultaneous infection) mice at day 14 and 21 post-infection. We report the degrees
980 of freedom (df), and the F and p values. N = 96 individuals.

Source of variation	**df**	**F**	**P**
Infection	2,90	19.01	<0.0001
Time	1,90	0.79	0.3755
Time*Infection	2,90	13.89	<0.0001

981

982

983

984 **Figure legends**

985

986 Figure 1. Schematic view of the experimental setup and groups. Non-infected (group 1) and single (Hp,
987 Py) infected mice (groups 2 and 3) were monitored during 35 days post-infection. One group of
988 coinfected mice (group 4) was simultaneously (the same day) infected with Py and Hp. The other
989 coinfection groups were either infected first with Hp (at day -7 or day -28) and then with Py (groups 5
990 and 6), or infected first with Py (at day -14 or day -28) and then with Hp (groups 7 and 8). Groups 4, 5
991 and 6 were monitored during 21 days post Py infection.

992

993 Figure 2. Changes in body mass over the course of the infection. Body mass is expressed as percent
994 variation with respect to body mass at day 0 [for the non-infected, single (Hp, Py) infected, and
995 simultaneous infection groups] or at the day of the second infection for the sequential coinfection
996 groups. a) Changes in body mass for non-infected and single (Hp, Py) infected mice; b) Changes in body
997 mass for non-infected, single Py infected and coinfected (Hp infecting first and simultaneous infection)
998 groups; c) Changes in body mass for non-infected, single Hp infected and coinfected (Py infecting first)
999 groups; d) Changes in body mass for coinfected groups depending on the order of the infection (Hp
1000 infecting first or Py infecting first). Dots represent the raw data, the lines represent the fit of a GLMM,
1001 and the shaded area around the line the 95% CI.

1002

1003 Figure 3. Changes in $\log_{10}$ transformed spleen mass (mg) over the course of the infection. a) Changes
1004 in spleen mass for non-infected and single (Hp, Py) infected mice; b) Changes in spleen mass for non-
1005 infected, single Py infected and coinfected (Hp infecting first and simultaneous infection) groups; c)
1006 Changes in spleen mass for non-infected, single Hp infected and coinfected (Py infecting first) groups;
1007 d) Changes in spleen mass for coinfected groups depending on the order of the infection (Hp infecting
1008 first or Py infecting first). Dots represent the raw data, the boxes represent the interquartile range
1009 (IQR), the horizontal lines the median, and whiskers the range of data within 1.5 the IQR.

1010 Figure 4. Effect of infection and coinfection on liver damage. a) Levels of aspartate aminotransferase
1011 (AST, ng/ml) in the plasma at day 21 p.i. in non-infected and single (Hp, Py) infected mice; b) AST level
1012 in plasma of non-infected, single Py infected and coinfected (Hp infecting first and simultaneous
1013 infection) groups at day 21 p.i.; c) AST level in plasma of non-infected, single Hp infected and coinfected
1014 (Py infecting first) groups at day 21 p.i.; d) AST level in plasma of coinfected mice, depending on the
1015 order of the infection (Hp infecting first or Py infecting first) at day 21 post-infection. Dots represent
1016 the raw data, the boxes represent the interquartile range (IQR), the horizontal lines the median, and
1017 whiskers the range of data within 1.5 the IQR.
1018
1019 Figure 5. Effect of infection and coinfection on host survival. a) Survival curves for non-infected and
1020 single (Hp, Py) infected mice; b) Survival curves for non-infected, single Py infected and coinfected (Hp
1021 infecting first and simultaneous infection) mice; c) Survival curves for non-infected, single Hp infected
1022 and coinfected (Py infecting first) mice; d) Survival curves for coinfected mice depending on the order
1023 of infection (Hp infecting first or Py infecting first). Crosses indicate censored observations.
1024
1025 Figure 6. Changes in parasitemia over the course of the infection. a) Changes in Py parasitemia
1026 (proportion of iRBCs counted using optical microscopy) in single infected mice over time; b) Changes
1027 in Py parasitemia (proportion of iRBCs) in single infected and coinfected (Hp infecting first and
1028 simultaneous infection) mice. Dots represent the raw data, the lines represent the fit of the GLMM,
1029 and the shaded area around the line the 95% CI.
1030
1031 Figure 7. Effect of infection and coinfection on RBCs. a) Changes in RBC counts measured by
1032 hematology analyzer for non-infected and single (Hp, Py) infected mice; b) Changes in RBCs for non-
1033 infected, single Py infected and coinfected (Hp infecting first and simultaneous infection) groups. Dots
1034 represent the raw data, the lines represent the fit of the GLMM, and the shaded area around the line
1035 the 95% CI. c) Levels of erythropoietin (EPO, log ng/ml) in the plasma assessed by ELISA at day 14 and

1036 21 p.i. in non-infected, single Py infected and coinfected (Hp infecting first and simultaneous infection)
1037 mice. Dots represent the raw data, the boxes represent the interquartile range (IQR), the horizontal
1038 lines the median, and whiskers the range of data within 1.5 the IQR; d) Changes in mean globular
1039 volume (MGV, fL) assessed by hematology analyzer for non-infected and single (Hp, Py) infected mice;
1040 e) Changes in MVG for non-infected, single Py infected and coinfected (Hp infecting first and
1041 simultaneous infection) groups. Dots represent the raw data, the lines represent the fit of the GLMM,
1042 and the shaded area around the line the 95% CI; f) Log-log plot of RBC counts on parasitemia for single
1043 Py infected and coinfected (Hp infecting first and simultaneous infection) groups. Dots represent the
1044 raw data, the lines represent the fit of the GLMM, and the shaded area around the line the 95% CI.
1045
1046 Figure 8. Effect of rEPO administration on the symptoms of the coinfection. a) Changes in body mass
1047 (g) over the course of the infection in mice that were infected with Hp at day -28 and with Py at day 0,
1048 and treated with rEPO or left as control; b) Changes in RBC counts assessed by hematology analyzer in
1049 coinfected mice treated with EPO or left as control. Dots represent the raw data, the lines represent
1050 the fit of the GLMM, and the shaded area around the line the 95% CI; c) Survival of coinfected mice
1051 treated with rEPO or left as control; d) Log-log plot of RBC counts on parasitemia for single Py infected
1052 mice and coinfected (infected with Hp at day -28 and with Py at day 0) mice treated with rEPO. Dots
1053 represent the raw data, the lines represent the fit of the GLMM, and the shaded area around the line
1054 the 95% CI.
1055
1056 Figure 9. Effect of infection and coinfection on heme detoxification. a) Fold change of *Hmox1* mRNA in
1057 spleen at day 14 p.i. in single Py infected and coinfected (Hp infecting first and simultaneous infection)
1058 groups; b) Levels of Heme oxygenase-1 in the plasma (log ng/ml) at day 14 and 21 p.i. in non-infected,
1059 single Py infected and coinfected (Hp infecting first and simultaneous infection) groups; c) Proportion
1060 of $CD163^{+}$ within $F4/80^{+}$ $CD11b^{-}$ cells analyzed by flow cytometry at day 14 and 21 p.i. in non-infected,
1061 single Py infected and coinfected (Hp infecting first and simultaneous infection) groups; d) Mean

1062 fluorescence intensity (arbitrary fluorescence units) of CD163 at day 14 and 21 p.i. in non-infected,
1063 single Py infected and coinfected (Hp infecting first and simultaneous infection) groups. Dots represent
1064 the raw data, the boxes represent the interquartile range (IQR), the horizontal lines the median, and
1065 whiskers the range of data within 1.5 the IQR.
1066
1067 Figure 10. Effect of infection and coinfection on cytokine expression. Fold change of a) IFN-γ, b) IL-10,
1068 c) TGF-β1 mRNA levels in spleen at day 3 and 14 p.i. in single Py infected and coinfected (Hp infecting
1069 first and simultaneous infection) groups. Dots represent the raw data, the boxes represent the
1070 interquartile range (IQR), the horizontal lines the median, and whiskers the range of data within 1.5
1071 the IQR.
1072
1073 Figure 11. Effect of infection and coinfection on Treg expansion and immunosuppressive function. a)
1074 Proportion of $FoxP3^+$ within $CD4^+$ T cells analyzed by flow cytometry over the course of the infection
1075 in non-infected, single Py infected and coinfected (Hp infecting first and simultaneous infection) mice;
1076 b) Proportion of $CTLA\text{-}4^+$ within $FoxP3^+$ $CD4^+$ T cells analyzed by flow cytometry over the course of the
1077 infection in non-infected, single Py infected and coinfected (Hp infecting first and simultaneous
1078 infection) mice. Dots represent the raw data, the boxes represent the interquartile range (IQR), the
1079 horizontal lines the median, and whiskers the range of data within 1.5 the IQR.
1080
1081 Figure 12. Immunophenotyping of spleen over the course of the infection. Principal component
1082 analysis (PCA) on the proportion of 20 immune cell populations at day 3 (a,d), 14 (b,e), 21 (c,f) p.i. in
1083 non-infected, single Py infected, and coinfected (Hp infecting first and simultaneous infection) hosts.
1084 We report the loadings of the 20 variables on the first two components of the PCA at each sampling
1085 day (a,b,c); the position of each individual host in the bivariate space defined by the PC1 and PC2,
1086 according to their experimental group (d,e,f); the scores on the PC1 (g) and PC2 (h) for the three

1087 experimental groups. For g) and h), dots represent the raw data, the boxes represent the interquartile
1088 range (IQR), the horizontal line the median, and whiskers the range of data within 1.5 the IQR.
1089
1090 Figure 13. Effect of infection and coinfection on Th2 and $CD8^+$ T cells. a) Proportion of GATA-3^+ within
1091 $CD4^+$ T cells and b) proportion of $CD8^+$ within $CD3^+$ T cells analyzed by flow cytometry over the course
1092 of the infection in non-infected, single Py infected and coinfected (Hp infecting first and simultaneous
1093 infection) hosts. Dots represent the raw data, the boxes represent the interquartile range (IQR), the
1094 horizontal lines the median, and whiskers the range of data within 1.5 the IQR.
1095
1096 Figure 14. Effect of infection and coinfection on $CD8^+$ T cell exhaustion. a) Proportion of CTLA-4^+ within
1097 $CD8^+$ T cells, b) LAG-3^+ within $CD8^+$ T cells, c) PD-1^+ within $CD8^+$ T cells analyzed by flow cytometry at
1098 day 14 and 21 p.i. in non-infected, single Py infected and coinfected (Hp infecting first and
1099 simultaneous infection) hosts. Dots represent the raw data, the boxes represent the interquartile
1100 range (IQR), the horizontal lines the median, and whiskers the range of data within 1.5 the IQR.
1101
1102 Figure 15. Correlation between the $CD4^+/CD8^+$ ratio at day 14 and 21 p.i. and the mortality rate in non-
1103 infected, single Py infected and coinfected (Hp infecting first and simultaneous infection) hosts.
1104 Mortality refers to the proportion of hosts reaching the experimental end points within groups. Dots
1105 represent the raw data, the line a linear regression fit and the band the 95% CI of the slope.
1106

Figure 1

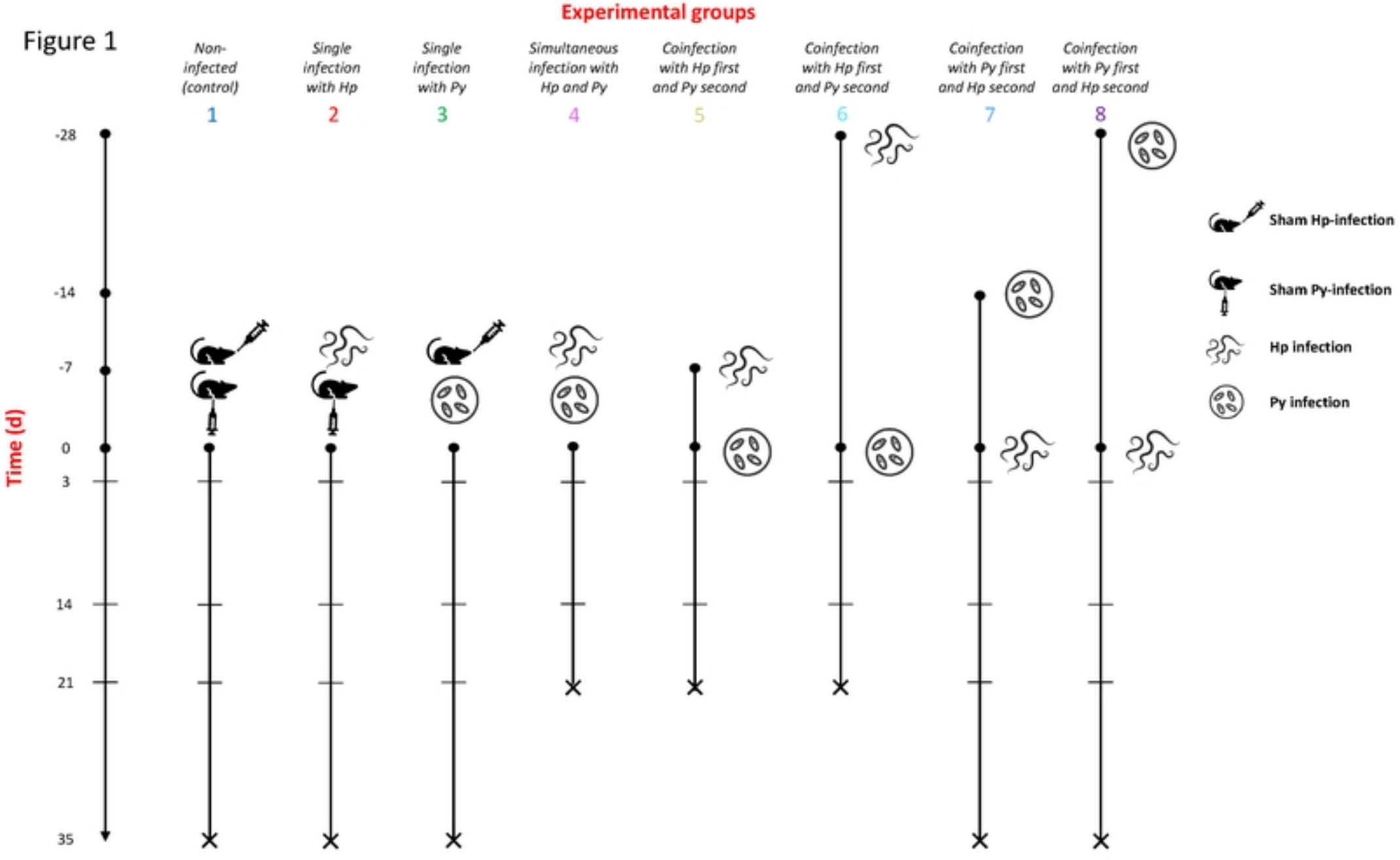
Experimental groups
Non-infected (control)
1
Single infection with Hp
2
Single infection with Py
3
Simultaneous infection with Hp and Py
4
Coinfection with Hp first and Py second
5
Coinfection with Hp first and Py second
6
Coinfection with Py first and Hp second
7
Coinfection with Py first and Hp second
8
Time (d)
-28
-14
-7
0
3
14
21
35
Sham Hp-infection
Sham Py-infection
Hp infection
Py infection

Figure 2

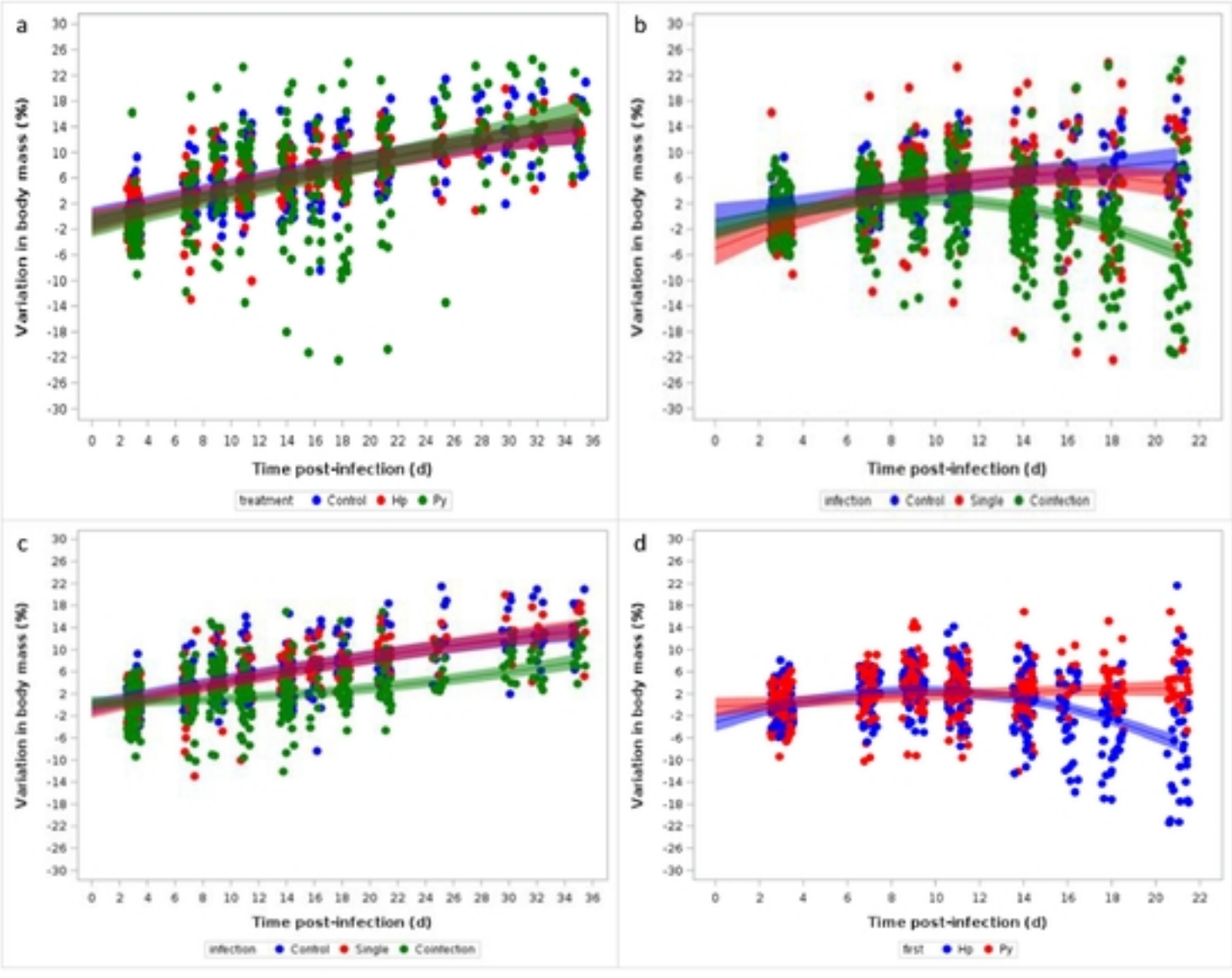
a
b
c
d
Variation in body mass (%)
Time post-infection (d)
treatment Control Hp Py
infection Control Single Coinfection
first Hp Py

Figure 3

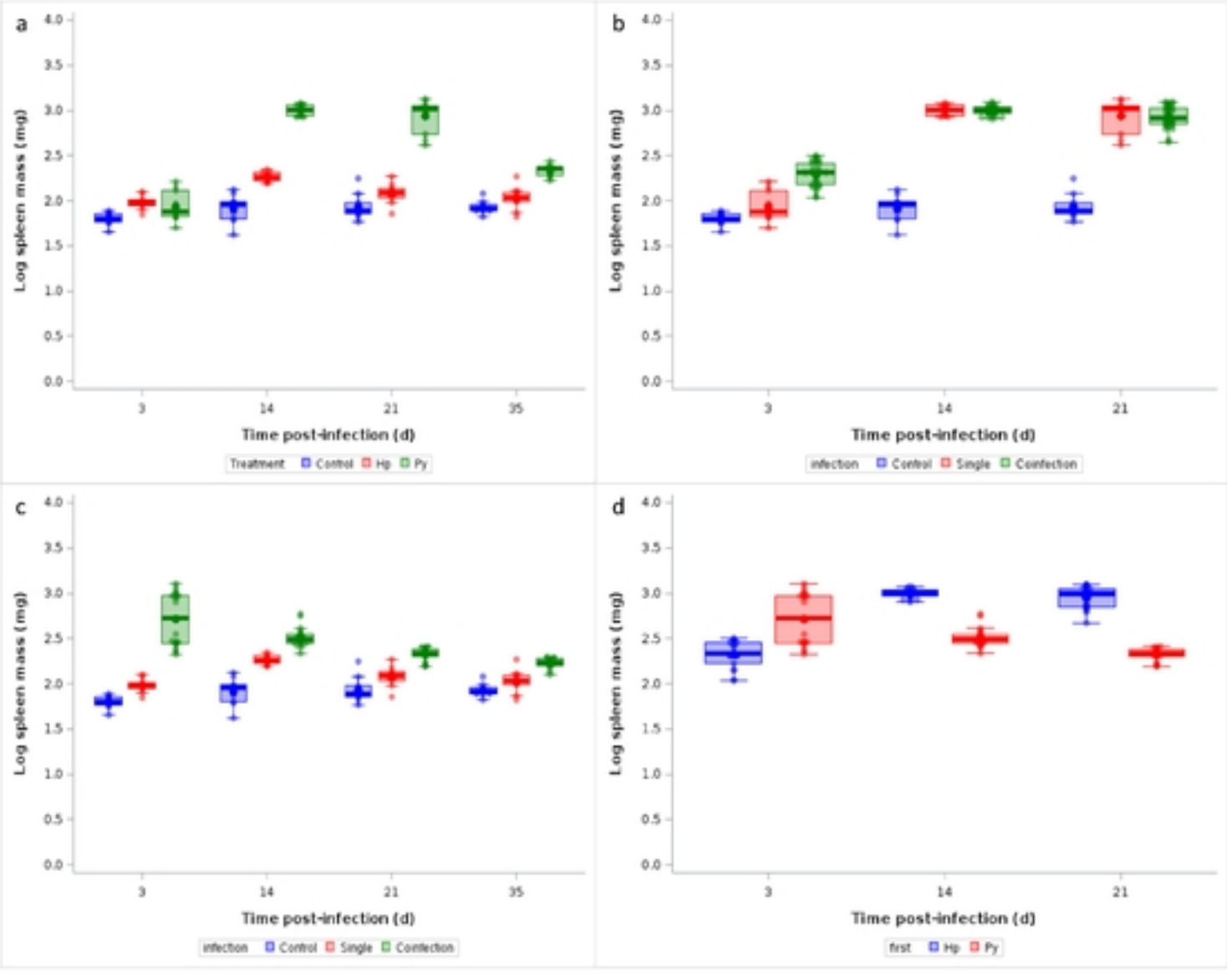
a
b
c
d
Log spleen mass (mg)
Time post-infection (d)
Treatment Control Hp Py
infection Control Single Coinfection
first Hp Py

Figure 4

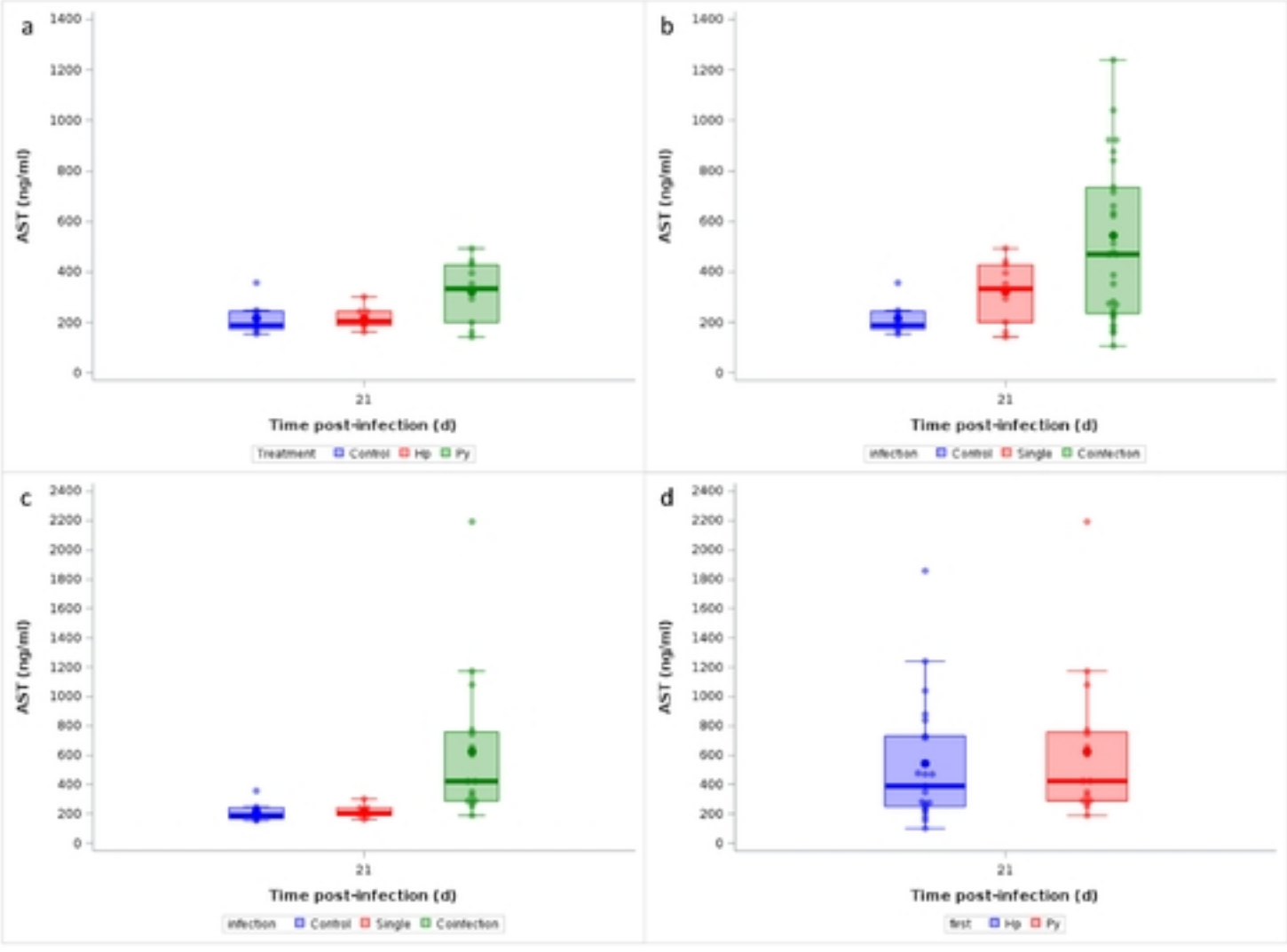
a
b
c
d
AST (ng/ml)
Time post-infection (d)
21
Treatment Control Hp Py
infection Control Single Coinfection
first Hp Py

Figure 5

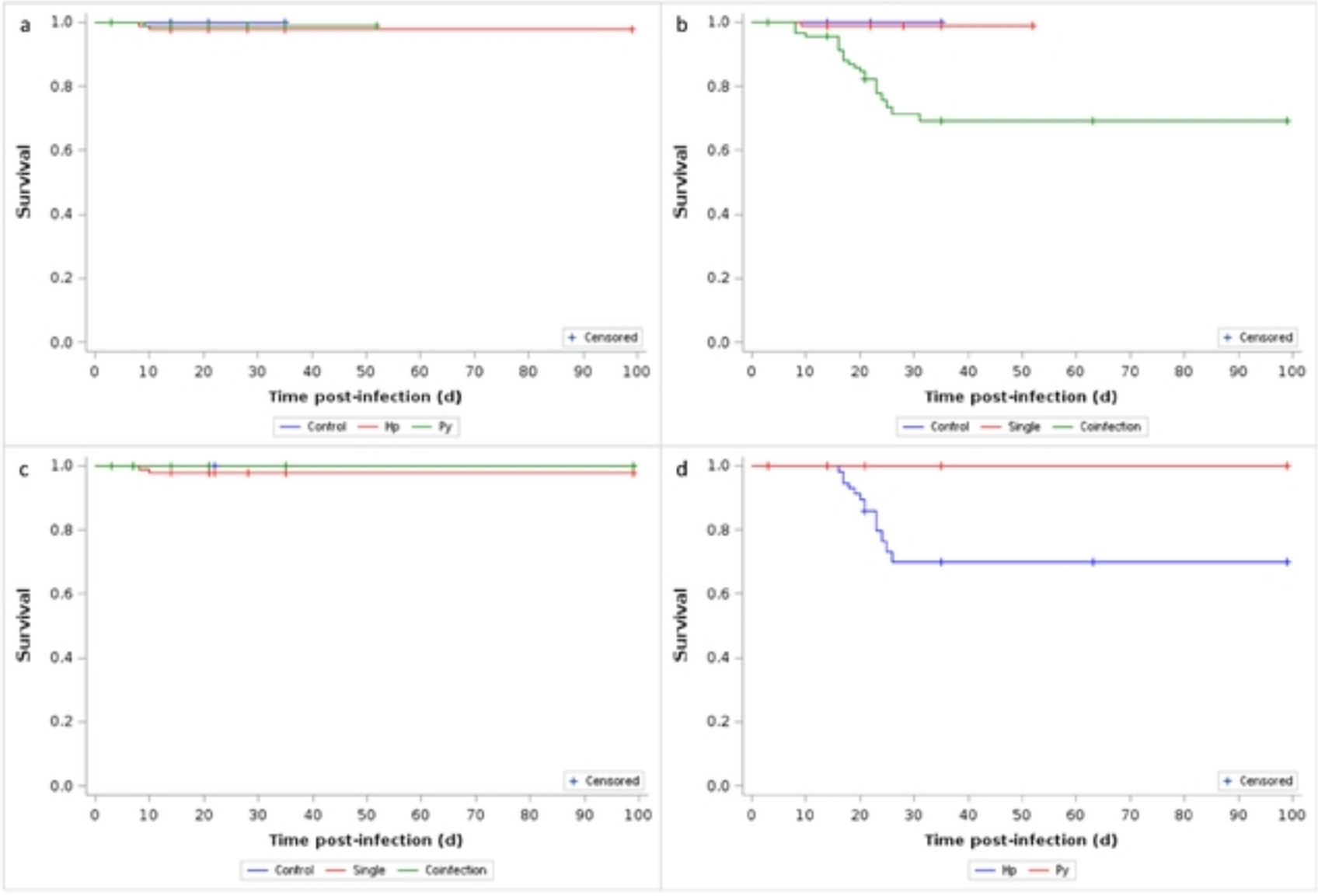
a
b
c
d
Survival
1.0
0.8
0.6
0.4
0.2
0.0
0
10
20
30
40
50
60
70
80
90
100
Time post-infection (d)
Censored
Control
Hp
Py
Single
Coinfection

Figure 6

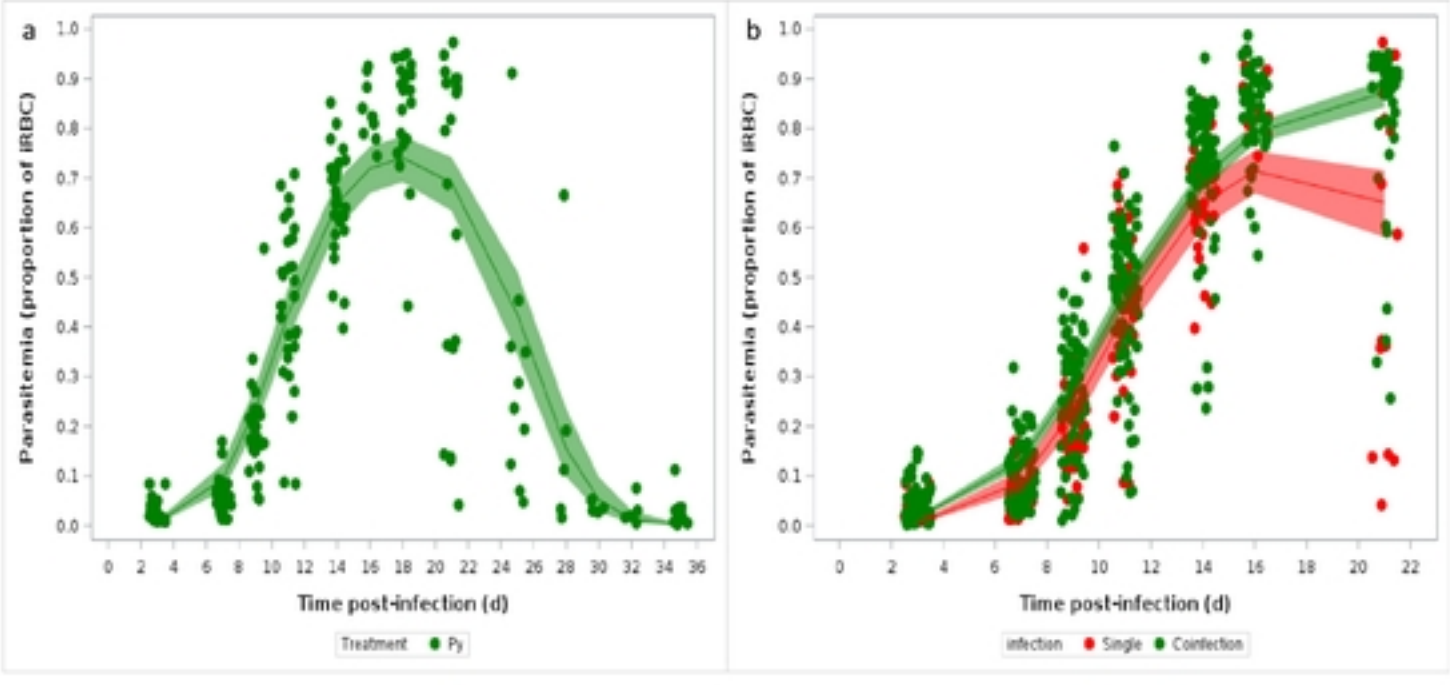
a
Parasitemia (proportion of iRBC)
Time post-infection (d)
Treatment
Py
b
Parasitemia (proportion of iRBC)
Time post-infection (d)
infection
Single
Coinfection

Figure 7

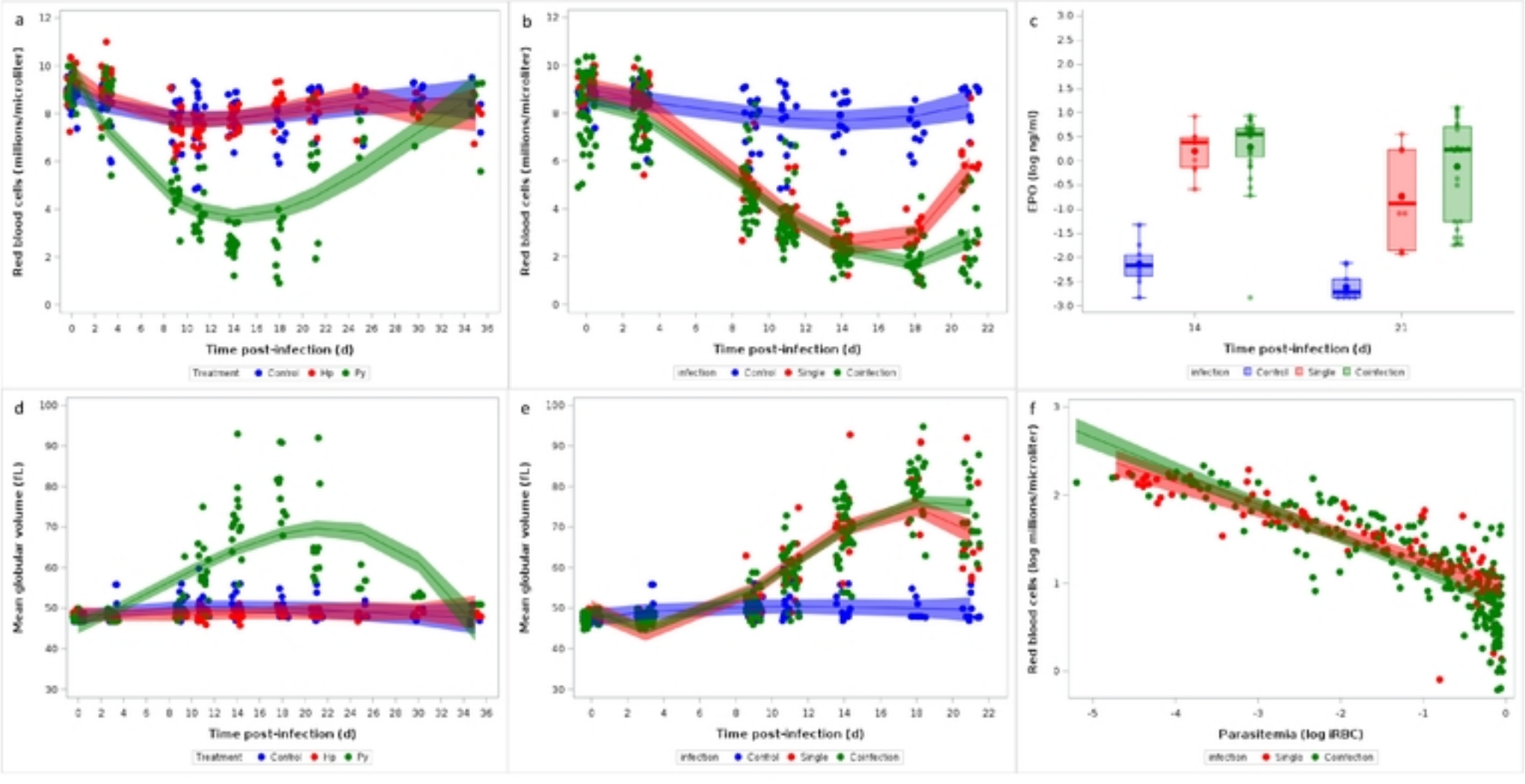
a
Red blood cells (millions/microliter)
Time post-infection (d)
Treatment Control Hp Py
b
Red blood cells (millions/microliter)
Time post-infection (d)
Infection Control Single Coinfection
c
EPO (log ng/ml)
Time post-infection (d)
Infection Control Single Coinfection
d
Mean globular volume (fL)
Time post-infection (d)
Treatment Control Hp Py
e
Mean globular volume (fL)
Time post-infection (d)
Infection Control Single Coinfection
f
Red blood cells (log millions/microliter)
Parasitemia (log iRBC)
Infection Single Coinfection

Figure 8

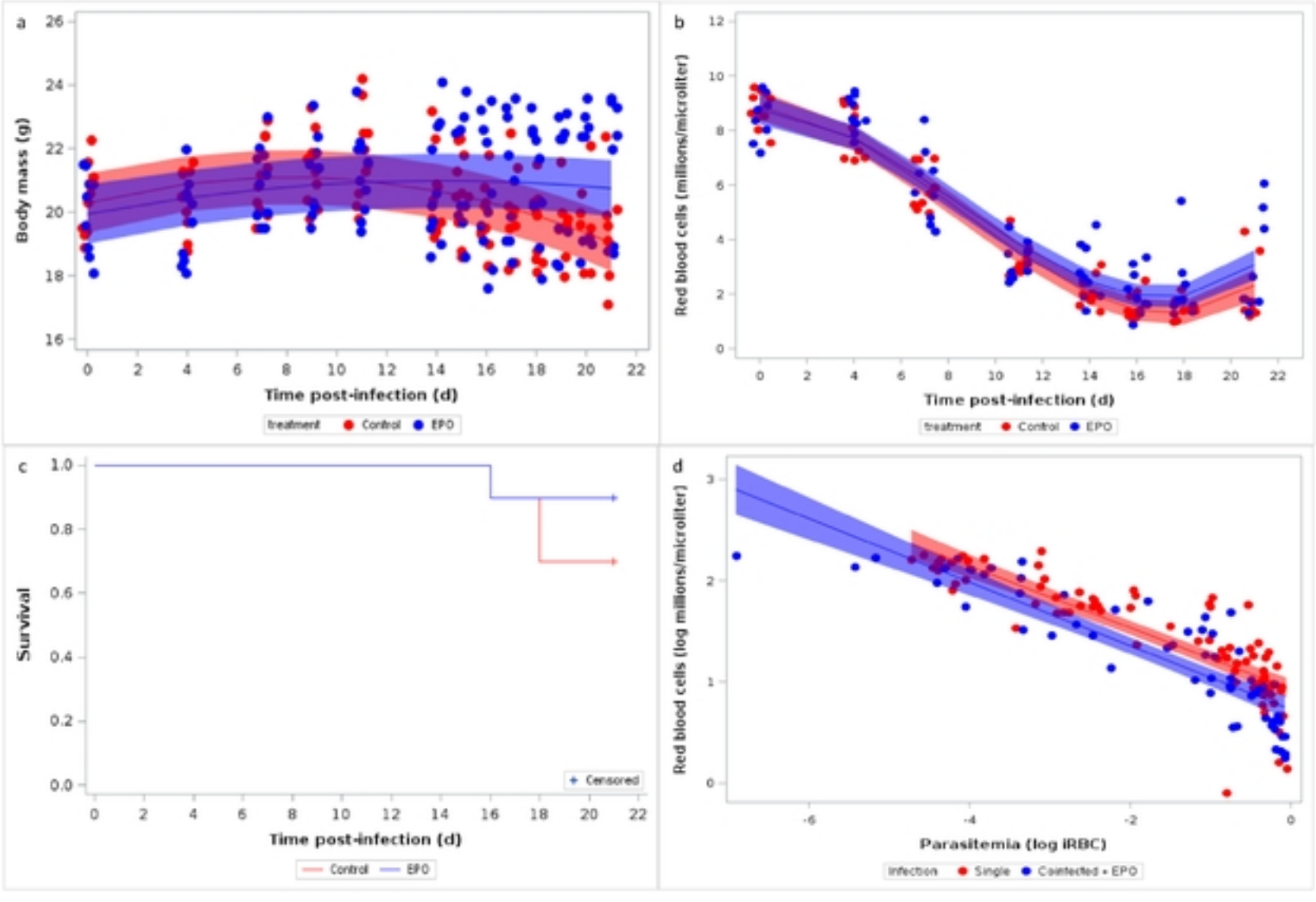
a
Body mass (g)
Time post-infection (d)
treatment Control EPO
b
Red blood cells (millions/microliter)
Time post-infection (d)
treatment Control EPO
c
Survival
Time post-infection (d)
Censored
Control EPO
d
Red blood cells (log millions/microliter)
Parasitemia (log iRBC)
Infection Single Coinfected + EPO

Figure 9

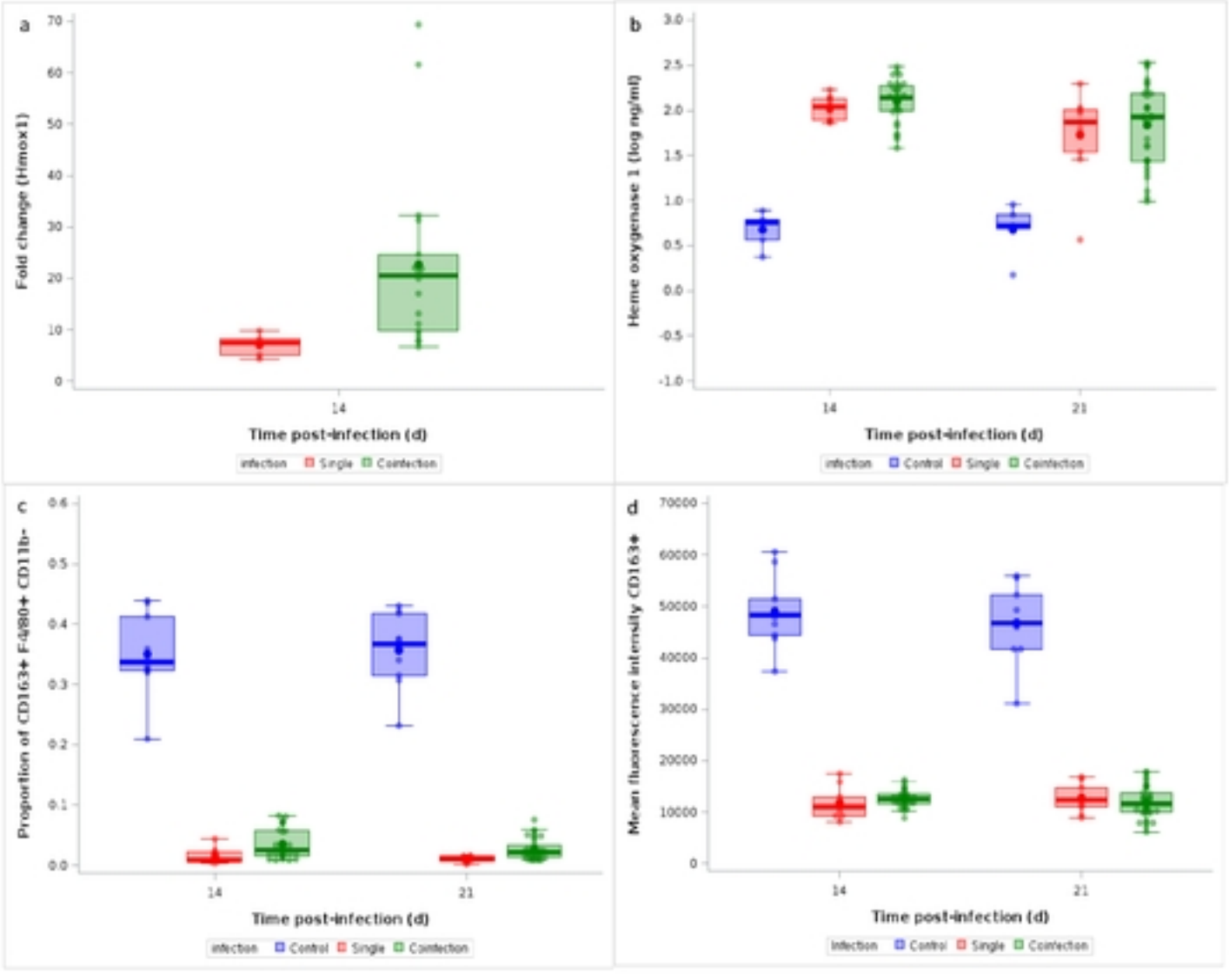
a
Fold change (Hmox1)
Time post-infection (d)
infection Single Coinfection
b
Heme oxygenase 1 (log ng/ml)
Time post-infection (d)
infection Control Single Coinfection
c
Proportion of CD163+ F4/80+ CD11b-
Time post-infection (d)
infection Control Single Coinfection
d
Mean fluorescence intensity CD163+
Time post-infection (d)
infection Control Single Coinfection

Figure 10

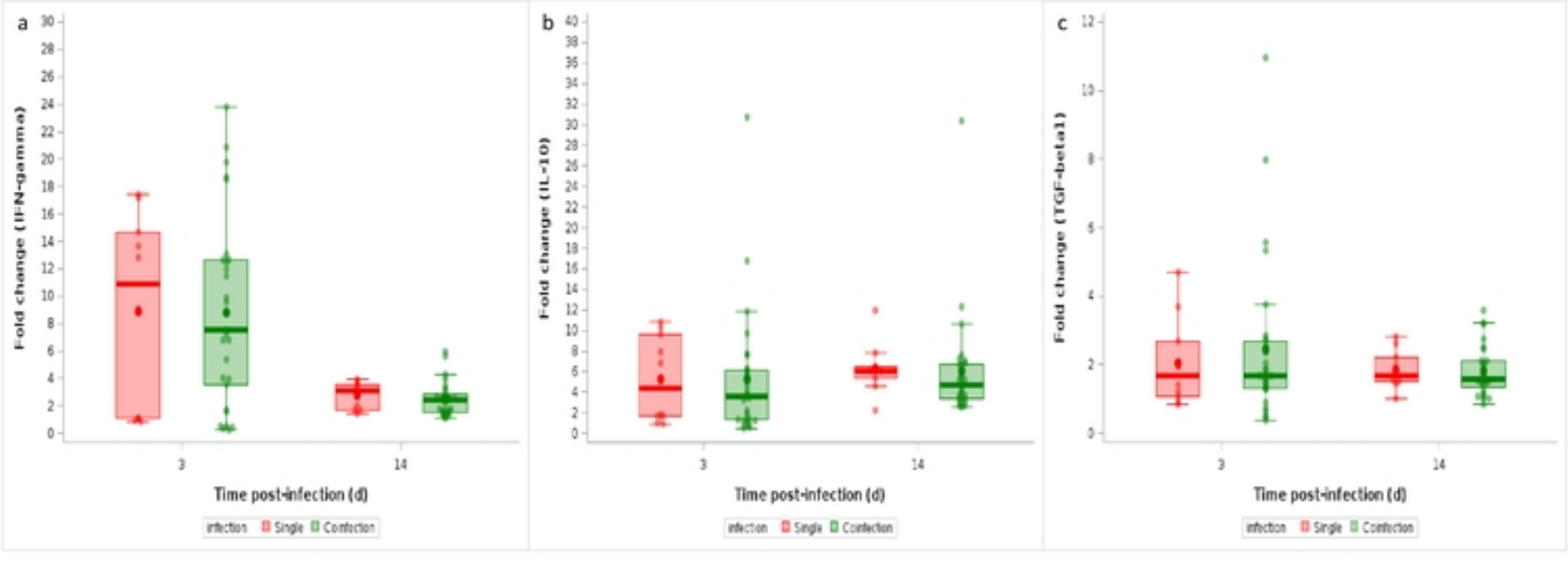
a
Fold change (IFN-gamma)
Time post-infection (d)
infection Single Coinfection
b
Fold change (IL-10)
Time post-infection (d)
infection Single Coinfection
c
Fold change (TGF-beta1)
Time post-infection (d)
infection Single Coinfection

Figure 11

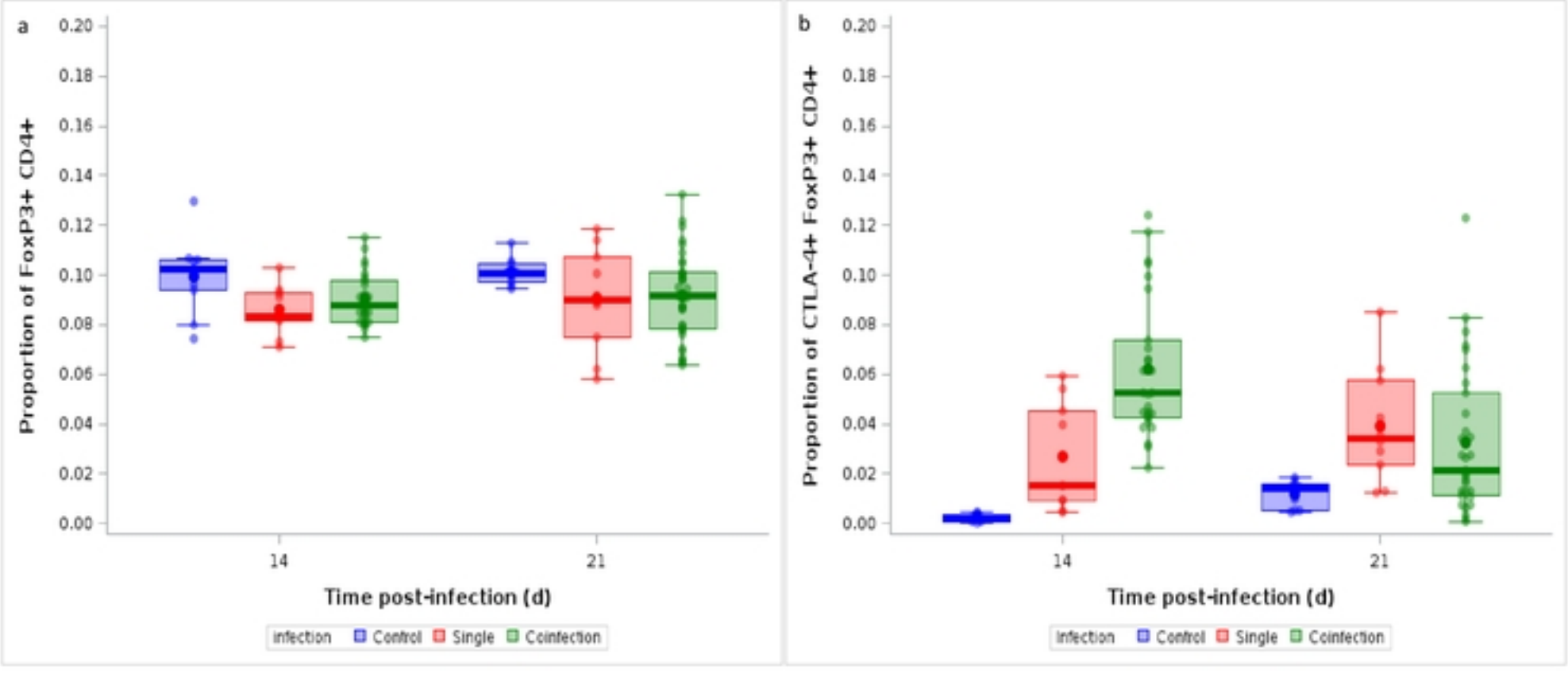
a
Proportion of FoxP3+ CD4+
0.20
0.18
0.16
0.14
0.12
0.10
0.08
0.06
0.04
0.02
0.00
14
21
Time post-infection (d)
Infection
Control
Single
Coinfection
b
Proportion of CTLA-4+ FoxP3+ CD4+
0.20
0.18
0.16
0.14
0.12
0.10
0.08
0.06
0.04
0.02
0.00
14
21
Time post-infection (d)
Infection
Control
Single
Coinfection

Figure 12

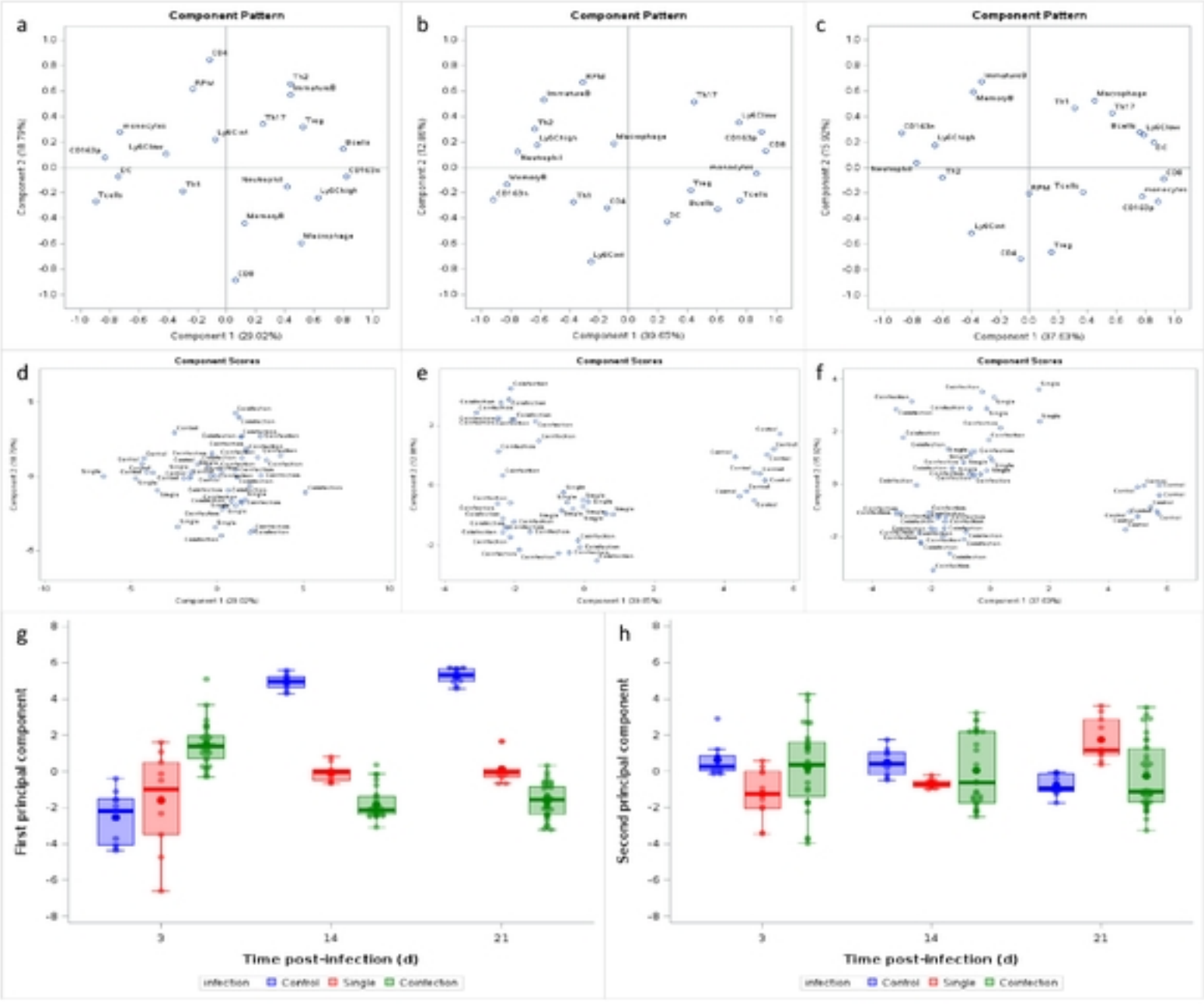
a
Component Pattern
Component 1 (29.02%)
Component 2 (18.79%)
b
Component Pattern
Component 1 (30.65%)
Component 2 (12.86%)
c
Component Pattern
Component 1 (37.63%)
Component 2 (15.90%)
d
Component Scores
e
Component Scores
f
Component Scores
g
First principal component
Time post-infection (d)
3
14
21
infection Control Single Coinfection
h
Second principal component
Time post-infection (d)
3
14
21
infection Control Single Coinfection

Figure 13

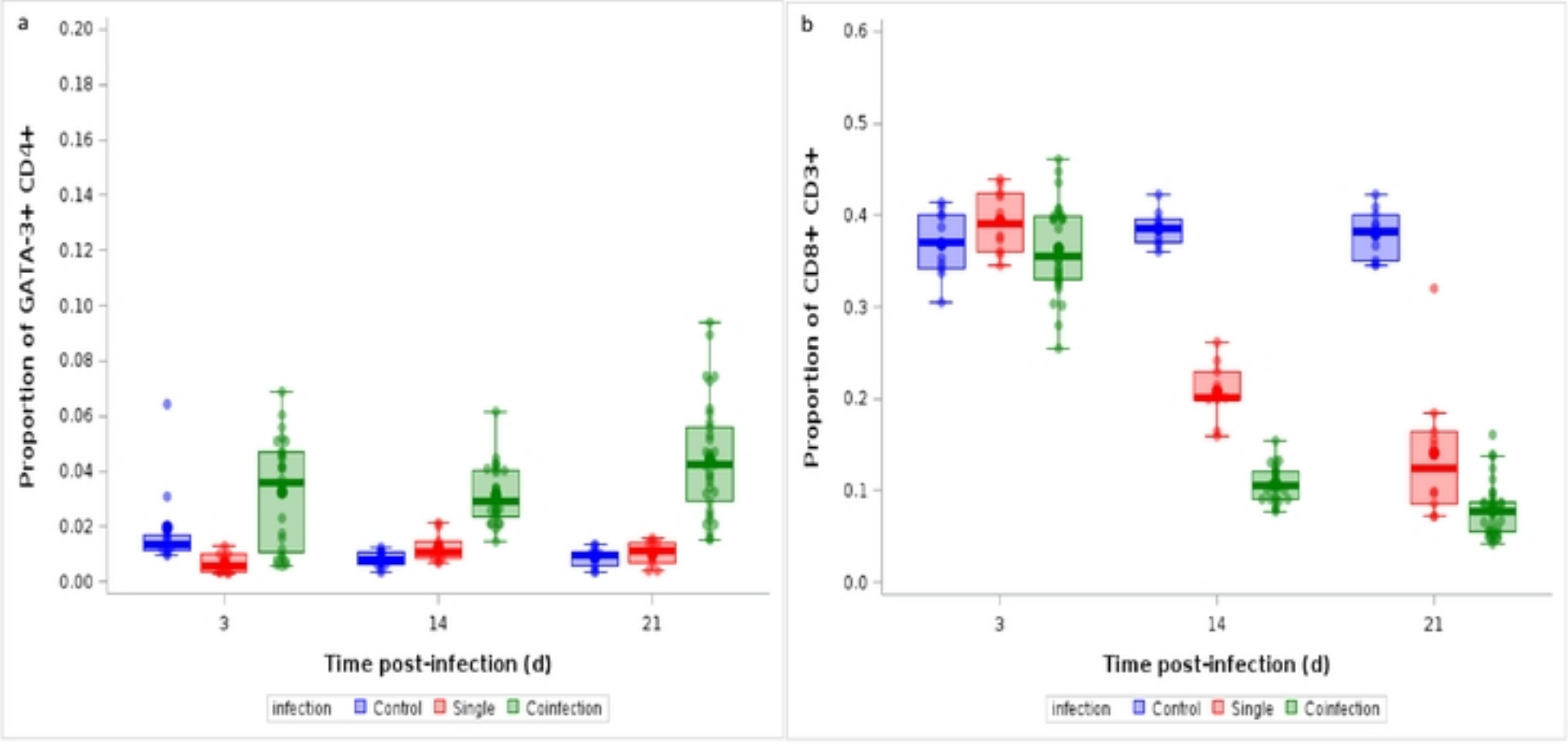
a
Proportion of GATA-3+ CD4+
0.20
0.18
0.16
0.14
0.12
0.10
0.08
0.06
0.04
0.02
0.00
3
14
21
Time post-infection (d)
infection Control Single Coinfection
b
Proportion of CD8+ CD3+
0.6
0.5
0.4
0.3
0.2
0.1
0.0
3
14
21
Time post-infection (d)
infection Control Single Coinfection

Figure 14

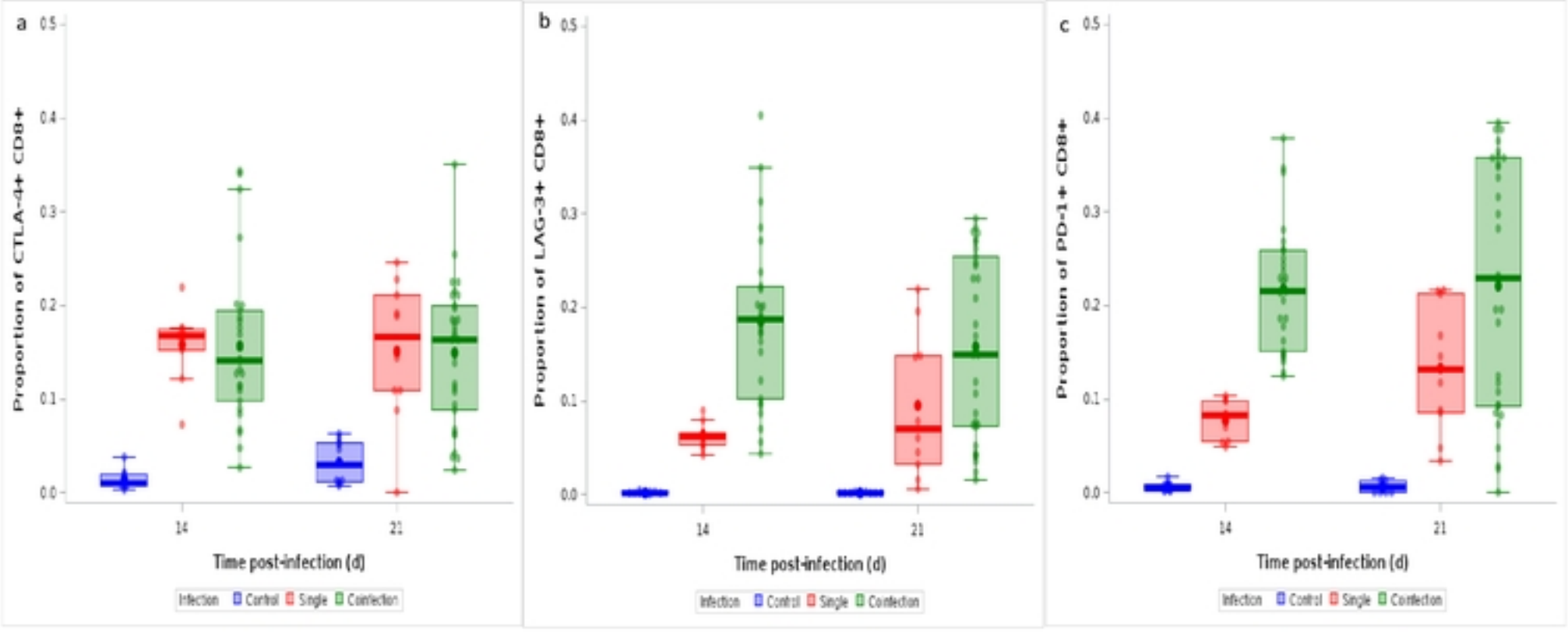
a
b
c
Proportion of CTLA-4+ CD8+
Proportion of LAG-3+ CD8+
Proportion of PD-1+ CD8+
0.0
0.1
0.2
0.3
0.4
0.5
14
21
Time post-infection (d)
Infection
Control
Single
Coinfection

Figure 15

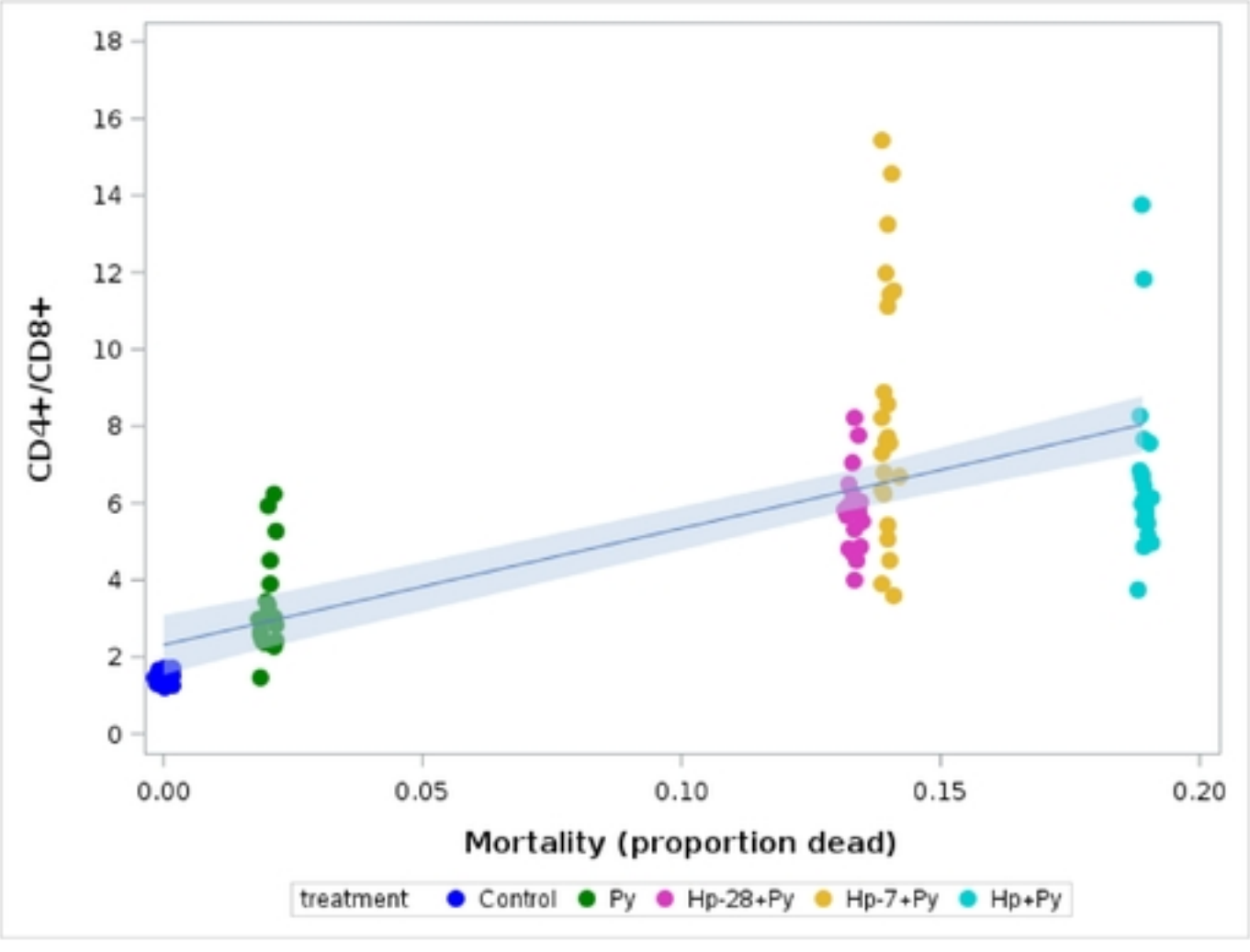
CD4+/CD8+
18
16
14
12
10
8
6
4
2
0
0.00
0.05
0.10
0.15
0.20
Mortality (proportion dead)
treatment
Control
Py
Hp-28+Py
Hp-7+Py
Hp+Py